GEORGIA DOT RESEARCH PROJECT 21-08

Final Report

STUDY ON SPECTRUM OPTIONS FOR GDOT'S CONNECTED VEHICLE INFRASTRUCTURE

Office of Performance-based Management and Research
600 West Peachtree Street NW | Atlanta, GA 30308

April 2024

TECHNICAL REPORT DOCUMENTATION PAGE

1. Report No.: FHWA 211108	2. Government Accession No.: N/A	3. Recipient's Catalog No.: N/A
4. Title and Subtitle: Study on Spectrum Options for GDOT's Connected Vehicle Infrastructure		5. Report Date: April 2024
		6. Performing Organization Code: N/A
7. Author(s): Seungmo Kim, Associate Professor, Georgia Southern University		8. Performing Organization Report No.: 21-08
9. Performing Organization Name and Address: Georgia Southern University Research and Service Foundation, Inc 261 Forest Drive Statesboro, GA.30458-8005		10. Work Unit No.: N/A
		11. Contract or Grant No.: PI# 0016970
12. Sponsoring Agency Name and Address: Georgia Department of Transportation Office of Performance-based Management and Research 600 West Peachtree St. NW Atlanta, GA 30308		13. Type of Report and Period Covered: Final - 04/27/2022 – 04/27/2024
		14. Sponsoring Agency Code: N/A
15. Supplementary Notes: Conducted in cooperation with the U.S. Department of Transportation, Federal Highway Administration.		

16. Abstract:

Vehicle-to-everything (V2X) communications are expected to take a critical role in a variety of transportation safety applications in connected and autonomous vehicle environment. However, Dedicated Short-Range Communications (DSRC), one of the representative technologies implementing the V2X communications, is encountering challenges due to the re-allocation of the 5.9 GHz spectrum by the Federal Communications Commission (FCC). The state of Georgia is leading the nation in the deployment of connected vehicle infrastructure with thousands of infrastructure units connecting vehicles based on DSRC. This project aimed at measuring the impact of the spectrum re-allocation on the performance of the Georgia's connected vehicle infrastructure. The project's particular technical focuses were to (i) model the performance of a DSRC system and (ii) design a protocol to improve the DSRC performance, under the FCC's reform of the 5.9 GHz band.

17. Keywords: Connected vehicles, 5.9 GHz band reform, DSRC, C-V2X, U.S. FCC	18. Distribution Statement: No Restriction

19. Security Classification (of this report): Unclassified	20. Security Classification (of this page): Unclassified	21. No. of Pages: 95	22. Price: Free

Form DOT 1700.7 (8-72) Reproduction of completed page authorized.

GDOT Research Project 21-08

Final Report

STUDY ON SPECTRUM OPTIONS FOR GDOT'S CONNECTED VEHICLE INFRASTRUCTURE

By

Seungmo Kim, Ph.D
Associate Professor, Department of Electrical and Computer Engineering
Georgia Southern University

Contract with
Georgia Department of Transportation

In cooperation with
U.S. Department of Transportation
Federal Highway Administration

April 2024

SI* (MODERN METRIC) CONVERSION FACTORS

APPROXIMATE CONVERSIONS TO SI UNITS

Symbol	When You Know	Multiply By	To Find	Symbol
		LENGTH		
in	inches	25.4	millimeters	mm
ft	feet	0.305	meters	m
yd	yards	0.914	meters	m
mi	miles	1.61	kilometers	km
		AREA		
in^2	square inches	645.2	square millimeters	mm^2
ft^2	square feet	0.093	square meters	m^2
yd^2	square yard	0.836	square meters	m^2
ac	acres	0.405	hectares	ha
mi^2	square miles	2.59	square kilometers	km^2
		VOLUME		
fl oz	fluid ounces	29.57	milliliters	mL
gal	gallons	3.785	liters	L
ft^3	cubic feet	0.028	cubic meters	m^3
yd^3	cubic yards	0.765	cubic meters	m^3
		NOTE: volumes greater than 1000 L shall be shown in m^3		
		MASS		
oz	ounces	28.35	grams	g
lb	pounds	0.454	kilograms	kg
T	short tons (2000 lb)	0.907	megagrams (or "metric ton")	Mg (or "t")
		TEMPERATURE (exact degrees)		
^oF	Fahrenheit	5 (F-32)/9 or (F-32)/1.8	Celsius	^oC
		ILLUMINATION		
fc	foot-candles	10.76	lux	lx
fl	foot-Lamberts	3.426	$candela/m^2$	cd/m^2
		FORCE and PRESSURE or STRESS		
lbf	poundforce	4.45	newtons	N
lbf/in^2	poundforce per square inch	6.89	kilopascals	kPa

APPROXIMATE CONVERSIONS FROM SI UNITS

Symbol	When You Know	Multiply By	To Find	Symbol
		LENGTH		
mm	millimeters	0.039	inches	in
m	meters	3.28	feet	ft
m	meters	1.09	yards	yd
km	kilometers	0.621	miles	mi
		AREA		
mm^2	square millimeters	0.0016	square inches	in^2
m^2	square meters	10.764	square feet	ft^2
m^2	square meters	1.195	square yards	yd^2
ha	hectares	2.47	acres	ac
km^2	square kilometers	0.386	square miles	mi^2
		VOLUME		
mL	milliliters	0.034	fluid ounces	fl oz
L	liters	0.264	gallons	gal
m^3	cubic meters	35.314	cubic feet	ft^3
m^3	cubic meters	1.307	cubic yards	yd^3
		MASS		
g	grams	0.035	ounces	oz
kg	kilograms	2.202	pounds	lb
Mg (or "t")	megagrams (or "metric ton")	1.103	short tons (2000 lb)	T
		TEMPERATURE (exact degrees)		
^oC	Celsius	1.8C+32	Fahrenheit	^oF
		ILLUMINATION		
lx	lux	0.0929	foot-candles	fc
cd/m^2	$candela/m^2$	0.2919	foot-Lamberts	fl
		FORCE and PRESSURE or STRESS		
N	newtons	0.225	poundforce	lbf
kPa	kilopascals	0.145	poundforce per square inch	lbf/in^2

Table of Contents

List of Figures

List of Tables

List of Abbreviations and Symbols

Abbreviation / Symbol	Meaning
3GPP	The 3rd-Generation Partnership Project
BSM	Basic safety message
C-V2X	Cellular vehicle-to-everything communications
CBR	Channel busy ratio
CV	Connected vehicle
CW	Contention window
DSRC	Dedicated short-range communications
FCC	The United States Federal Communications Commission
GDOT	Georgia Department of Transportation
ITS	Intelligent transportation system
LTE	Long Term Evolution
MAC	Medium access control
MCS	Modulation and coding scheme
PDB	Packet delay budget
PDR	Packet delivery rate
PHY	Physical layer
PPP	Poisson point process
PPPP	ProSe per-packet priorities
QPSK	Quadrature phase shift keying
RAT	Radio access technology
RX	Receiver
SDR	Software-defined radio
TX	Transmitter
USDOT	The United States Department of Transportation
USRP	Universal Software Radio Peripheral
V2I	Vehicle to infrastructure
V2V	Vehicle to vehicle
V2X	Vehicle to everything

Executive Summary

Vehicle-to-everything (V2X) communications are expected to take a critical role in a variety of transportation safety applications in connected vehicle environment. However, Dedicated Short-Range Communications (DSRC), one of the representative technologies implementing V2X communications, has been supplanted by Cellular V2X (C-V2X) as the primary connected vehicle communications technology due to the re-allocation of the 5.9 GHz spectrum by the Federal Communications Commission (FCC). The state of Georgia is leading the nation in the deployment of connected vehicle infrastructure with more than 1,700 roadside units (RSUs) operating in DSRC. This project aims at measuring the impact of the spectrum re-allocation on the performance of the Georgia's connected vehicle infrastructure. This project's particular technical focus is to investigate various solutions to resolve the bandwidth reduction at the 5.9 GHz band. To wit, the project proposes to delve into the feasibility of the following options:

- Task 1: DSRC in Unlicensed Bands
- Task 2: DSRC in 4.9 GHz Public Safety Band
- Task 3: Transition to cellular V2X (C-V2X)
- Task 4: The Intelligent Transportation Society of America (ITSA) 30 MHz Application Map

The aforementioned four options form the respective four research tasks, the final result of which will be reported in what follows.

Chapter 1. Introduction

Background

Connected vehicles are no longer a futuristic dream coming out of science fiction, but they are swiftly taking a bigger part of one's everyday life. One of the key technologies actualizing the connected vehicles is vehicle-to-everything (V2X) communications.

V2X communications have the potential to significantly reduce the occurrence of vehicle crashes and associated fatalities, as highlighted by the US Department of Transportation in 2017 (US Department of Transportation 2017). These communications play a central role in intelligent transportation systems (ITS) for connected vehicle environments. Currently, Dedicated Short Range Communications (DSRC) and Cellular-V2X (C-V2X) are the two main radio access technologies (RATs) enabling V2X communications. DSRC operates exclusively in the 5.9 GHz band, designated for ITS applications in many countries. In contrast, C-V2X can operate in the 5.9 GHz band and the licensed bands of cellular operators (Wang, Mao and Gong 2017).

DSRC has been tested for safety-critical applications in many countries for a longer duration, which boasts a significant advantage of being a proven technology. Capitalizing on this, over 5,315 roadside units (RSUs) operating in DSRC were deployed nationwide in the United States by November 2018, following the Federal Communications Commission's dedication of the 5.9 GHz band to DSRC in 1999. Despite the widespread deployment and proposed mandates by the National Highway Traffic Safety Administration (NHTSA) in 2016, there are still key issues to address to ensure the stable operation of DSRC (Kenney Nov. 2018, NHTSA 2016).

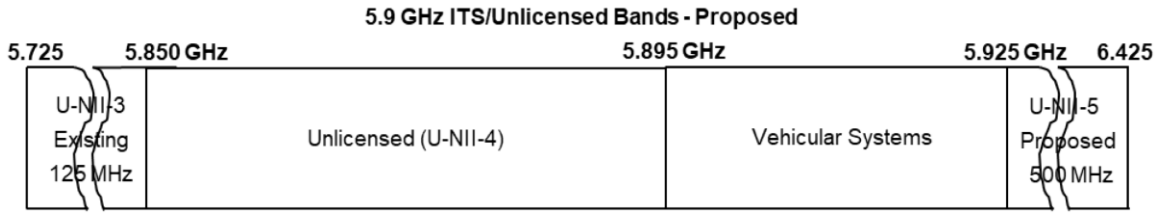

Figure 1. Illustration. FCC's proposed 5.9 GHz band reform

The FCC's 5.9 GHz Band Reform

Out of the 75 MHz of bandwidth in the 5.9 GHz band (i.e., 5.870-5.925 GHz), in December 2019, the U.S. FCC began to allocate the lower 45 MHz (i.e., 5.850-5.895 GHz) for unlicensed operations to support high-throughput broadband applications (e.g., Wireless Fidelity, or Wi-Fi) (US FCC Dec. 2019.). Figure 1 illustrates this proposed bandwidth reform. The key points of the reform are two-fold: (i) it leaves the upper 30 MHz (i.e., 5.895-5.925 GHz) for ITS operations; (ii) it dedicates the upper 20 MHz of the chunk (i.e., 5.905-5.925 GHz) for C-V2X.

According to this plan, DSRC is only allowed to use 10 MHz of spectrum (i.e., 5.895-5.905 GHz). It has never been studied nor tested if 10 MHz would suffice for the operation of the existing DSRC-based transportation safety infrastructure. The state of Georgia is a recognized national leader in the deployment of connected vehicle infrastructure, with considerable investment in DSRC. As such, it has become urgent to understand how much impact the FCC's 5.9 GHz band reform will be placed on the performance of Georgia's connected vehicle infrastructure.

Possible Bandwidth Contention with C-V2X

According to the FCC's 5.9 GHz band reform (US FCC Dec. 2019.), DSRC may need to coexist with C-V2X users in the upper 30 MHz (i.e., 5.895-5.925 GHz). The key technical challenge here is that C-V2X uses a different technology standard, and hence the technology is incompatible with DSRC-based operations. Based on the principal investigator (PI)'s recent investigation (Kim and Bennis 2019), on average 4.63 C-V2X vehicles can be affected by interference within a 10-MHz channel of DSRC. It implies that coexistence of 5 C-V2X vehicles may significantly degrade the performance of a DSRC system.

Literature Review

Stochastic Methods for Modeling the Performance of DSRC

For the general IEEE 802.11 standard, carrier-sense multiple access with collision avoidance (CSMA/CA) has been modeled as a two-dimensional Markov chain (Bianchi 1998). However, in DSRC, the contention window size does not get doubled even upon a packet collision, which simplifies the Markov chain structure.

The key difference in our model is that for basic safety messages (BSM) broadcast in a DSRC system, the probability of decrementing a backoff counter is not 1. Also, a Markov chain has been proposed to model the broadcast of safety messages in DSRC (Yin, Ma and Trivedi 2013); yet it does not take into account a packet expiration (EXP) during a backoff process. Further, there was another aspect about which the model did not describe completely accurately. According to the IEEE 802.11p-2010 standard (IEEE 2010), the fundamental access method of

the IEEE 802.11 medium access control (MAC) is a distributed coordination function (DCF), which shall be implemented in all stations (STAs). Investigating the CSMA/CA written in IEEE 802.11 MAC (Bianchi 1998) (IEEE 2016), the probability of transmission at the state of backoff being 0 still requires the probability of $1 - \text{Pb}$ for a transmission (where Pb denotes the probability of a slot being busy).

Also, the previous models suggested that analysis of 802.11p beaconing mechanism paid only little attention to the varying number of contending nodes (Yao, Rao and Liu 2013) and the restricted channel access of the control channel (CCH), i.e., Channel 178 (5.885-5.895 GHz) (Khabazian, Aissa and Mehmet-Ali 2013). Since the 802.11p MAC protocol is a contention-based scheme, the joint effect of the varying number of contending nodes and the restricted channel access may lead the network to perform quite differently (Lei and Rhee 2019). However, P_{tx}, the probability of a vehicle's making it through a backoff process, was overly simplified in the previous study (Lei and Rhee 2019), which limits the model's applicability. That is, while DSRC usually adopts an exponential backoff, the model overly simplified the probability as $P_{tx} = 2/(CW + 1)$, which can only be used when there is no exponential backoff (Bianchi 2000). Notice that CW stands for a "contention window," from which a STA chooses a backoff counter value.

Given the significance of an EXP in determining the performance of a DSRC system, the previous models cannot be considered as methods to precisely characterize the behavior of a safety message broadcast. In this work, we develop a new mathematical model that integrates those two factors.

DSRC Performance Measurement Metrics

Packet delivery rate (PDR) is one of the classical metrics that are used to measure the performance of a communications network. The PDR is defined as the ratio of data packets that are actually received at the receiver end to those which were originally sent by the sender. Besides the classical metrics, some other metrics have also been used to evaluate the performance of congestion control techniques. Examples include the probability of successful reception of beacon message (Torrent-Moreno, et al. 2009), update delay (Kloiber, et al. 2015) as the elapsed time between two consecutive BSMs successfully received from the same transmitter, a 95% Euclidean cutoff error (in meters) (Huang, et al. 2010), and information dissemination rate (IDR) (Fallah, et al. 2010).

Other metrics could be found in the literature as well. The inter-reception time (IRT) is a metric motivated from the need to display both successful and failed transmissions at once. A later work proposed an algorithm that adapts the frequency of BSM broadcast according to the IRT (Son and Park 2019). The key limitation of the metric is that it measures the BSM reception performance only at a single vehicle.

For that reason, this project adopts the PDR as the main metric in the evaluation of the performance of a DSRC network. In fact, compared to receiver vehicle-centric metrics, the PDR better serves our purpose of evaluating a system as an entirety rather than measuring the performance of a single vehicle. The key innovation of this project is that we provide an extensive mathematical analysis framework as well as a comprehensive computer simulation

framework. This distinguishes our work from other simulation-based work (ElBatt, et al. 2006) (Jornod, et al. 2019) (Almeida, et al. 2018) (Cheng, et al. 2017) (Khan, Hoang and Harri 2017) and experiment-based work (Liu, et al. 2016) (Rendaa, et al. 2016).

Inter-Technology Coexistence in the 5.9 GHz Band

The coexistence problem among dissimilar RATs in the 5.9 GHz band has been discussed in the literature: (i) between DSRC and Wi-Fi (S. Kim 2017) and (ii) between DSRC and Wi-Fi/C-V2X (Kim and Bennis 2019).

Modification of CSMA was proposed for relieving bandwidth contention among vehicles within an IEEE 802.11p network (Kim and Dessalgn 2019). A message prioritization scheme among different classes of vehicles was proposed for military vehicles over commercial ones (Kim and Dessalgn 2019). The key limitation was a relatively simple model for the stochastic geometry: a single junction of two 6-lane road segments. Such an urban model may lose generality when applied to more complicated scenarios.

Another reinforcement learning-based approach was proposed to address the dynamicity of a V2X networking environment (Kim and Kim 2020). Each vehicle needs to recognize the frequent changes of the surroundings and apply them to its networking behavior, which was formulated as a multi-armed bandit (MAB) problem. This reinforcement learning mechanism enabled a vehicle, without any external assistance, to (i) learn the environment, (ii) quantify the accident risk, and (iii) adapt its backoff counter according to the risk.

Chapter 2. Task 1: DSRC in Unlicensed Bands

Can Wi-Fi serve as an alternative to DSRC? This research explores the feasibility of Wi-Fi to support the V2X communications that DSRC used to serve. The key motivation of this work is the U.S. federal government's recent movement of removing DSRC from being permitted to operate in the 5.850-5.925 GHz spectrum, also known as "the 5.9 GHz band." The issue is that many of the current DSRC operators still desire to continue using this technology, concerned about transition costs. As such, this research suggests the operation of the safety-critical traffic applications via Wi-Fi, which shares key technical principles with the DSRC. In doing so, we identify as the key challenge the coexistence between the V2X and existing Wi-Fi users (which we call "V2X" and "Wi-Fi," respectively, throughout this research). Particularly, in a V2X network, it is not trivial to (i) control congestion and (ii) guarantee the successful delivery of a safety message. To this end, we propose a method to "lighten" the load of a V2X network. Technically, it is to allocate the backoff counter according to the level of an accident risk that a vehicle marks in each time slot. Simulation results show that the proposed mechanism (i) decreases the interference into the Wi-Fi users and hence (ii) increases the message delivery performance within the V2X network.

Background

Wi-Fi for V2X

The U.S. FCC began reallocation of the 5.9 GHz band (FCCUS 2019) wherein DSRC has been the long-time primary V2X technology. Interestingly, other regions of the world are going in a similar direction. For instance, Europe (5GCAR 2019) and China (5GAA 2019) are also

considering C-V2X as the primary V2X technology over DSRC. Nonetheless, many parties that have already deployed DSRC units are concerned of enormous cost transitioning to C-V2X due to the drastic technical dissimilarity between the two technologies (AASHTO 2019). This leads to a question: can Wi-Fi replace DSRC to serve V2X communications? This question is a valid one, particularly considering the technical similarity between DSRC and Wi-Fi (S. Y. LienD. 2017). As such, if one seeks an alternative technology for DSRC, it will be natural for one to think of Wi-Fi as one of the easiest options. Also, the idea does not violate any regulations. In fact, according to the U.S. FCC Part 15 Subpart C regulating the unlicensed wireless operations, the technical requirements (including the maximum transmit (TX) power of 30 dBm) are enough to support a V2X system.

V2X Access Enhancement

A key requirement of vehicle-to-vehicle (V2V) communications is the reliable delivery of safety messages. However, most unlicensed bands have already been experiencing increasing interference from neighboring devices and severe collisions from channel contention in a crowded wireless environment. Furthermore, as more connected vehicles are deployed, the number of exchanged messages will explode, which will likely deteriorate the message delivery performance. As such, the priority of transmitted information needs to be carefully defined to ensure that vehicles can obtain timely access to information that is critical to road safety. It naturally translates to a particular question: how can the priority be defined? This research proposes to base on the variance of speed of each vehicle.

Contributions

The contributions of this research are summarized as

- It provides an analytical framework for quantification of the inter-RAT interference (viz., Wi-Fi-to-V2X (W2V) and V2X-to-Wi-Fi (V2W) interference), with the outdoor-to-indoor (O2I) path loss as the key factor under the assumption of deploying Wi-Fi indoor and V2X outdoor.
- Discovering that W2V interference is far higher than V2W interference, we proceed to proposing a method to lighten the load of a V2X network, as a means to accomplish the latency requirements even with the presence of W2V interference. Specifically, this research proposes a novel backoff allocation mechanism where the vehicle with a higher risk takes a higher priority in access to the medium. The mechanism features direct applicability to other currently operated distributed V2X networking standards--e.g., IEEE 802.11p and C-V2X mode 4.
- This research presents a closed-form analysis framework for the performance of the proposed Wi-Fi-based V2X network. The framework features a precise Markov chain-based analysis taking into account the packet expiration and the over-the-air collision, which idiosyncratically becomes critical in a distributed V2X network unlike other IEEE 802.11-based technologies due to the dynamicity.

Related Work

Wi-Fi for V2X

We are not the first thinking of using Wi-Fi to deliver V2X signals. There were several prior studies that examined the feasibility of various versions of unlicensed technologies to support V2X communications: IEEE 802.11a (W.-Y. LinM.-W. 2010), IEEE 802.11b (GungorB. 2013) and IEEE 802.11ax (S. Y. LienD. 2017). However, none of the prior work considered the impacts of coexistence with the existing Wi-Fi users. Our work distinguishes itself by addressing this point: this research provides a detailed framework quantifying the interference between V2X and legacy Wi-Fi users.

V2X Access Enhancement

The enhanced distributed channel access (EDCA) (SongC. 2017) forms a main body of prior work as to enhancing the IEEE 802.11 MAC. However, this research particularly aims to increase the success rate of broadcasting safety messages by high driving-risk vehicles. We claim that the EDCA is not enough to achieve that purpose for the following reasons: (i) inefficiency with a higher traffic load (A. I. Abu-KhadrahA. 2017) and frequent changes in load (R. MoraesP. 2010); (ii) inefficiency in supporting fairness when a network requires diverse requirements (ChoS. 2013). After all, to guarantee the prioritization of high-risk vehicles in safety-critical applications, we need a more aggressive approach than the EDCA.

There have been other proposals focusing on enhancing the IEEE 802.11 MAC. In the current 802.11 MAC mechanism, the size of the contention window (CW) is dictated to take discrete

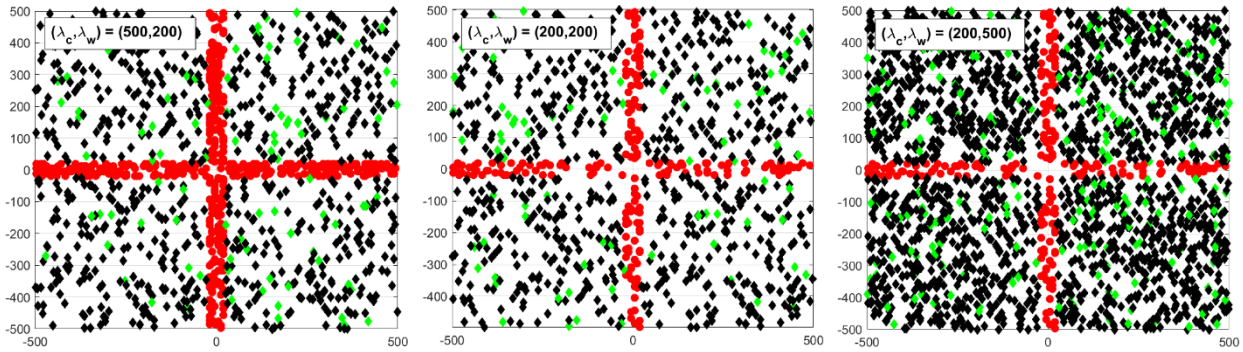

(a) More cars than Wi-Fi users (b) Equal density of cars and Wi-Fi users (c) More Wi-Fi users than cars

Figure 2. Density plot. A snapshot of relative traffic densities for V2X and Wi-Fi (Red dot for a V2X STA; Black dot for a Wi-Fi STA (indoor); Green dot for a Wi-Fi STA (outdoor))

values from a bounded finite set (LobiyalP. 2015). The limitations of this constraint have been investigated (M. KaracaS. 2017), to discover the limitation on the CW size in the main bottleneck in a dense network. Also, the binary exponential backoff (BEB) scheme has been found not to provide a satisfiable level of fairness due to little correlation between a backoff time and a CW (M. Al-HubaishiT. 2014). Furthermore, the IEEE 802.11 BEB mechanism produces a large variation in the backoff time (N. O. SongB. 2003). That is, every new packet after a successful delivery starts with CWmin, which may be too small for a heavy network load. It can easily lead to a higher level of network congestion. For this reason, the current BEB relies too heavily on the CW size, which makes itself less suitable for distributed networks (FapojuwoK. 2018).

In that context, modification of CSMA has been proposed for relieving bandwidth contention among vehicles within an IEEE 802.11p network (KimS, DessalgnT, Danger aware vehicular networking 2019). The inter-vehicle distance was selected as the factor representing the driving risk. In a similar context, a message prioritization scheme among different classes of vehicles was proposed for military vehicles over commercial ones (KimS, DessalgnT, Mitigation of

civilian-to-military interference in DSRC for urban operations 2019). The key limitation was a relatively simple model for the stochastic geometry: a single junction of two 6-lane road segments. Our work extends the model in such a way to extend the applicability to other scenarios.

System Model

This subsection presents key assumptions that this research establishes as an effort to precisely model the performance of the proposed V2X networking mechanism.

First, we characterize the *spatial separation* of Wi-Fi and V2X as follows. It is acknowledged that the current unlicensed RATs adopt spread spectrum techniques as an effort to alleviate the impact of interference. Distinguished from that, this research is focused on the spatial analysis when the Wi-Fi and V2X are deployed indoor and outdoor, respectively. In fact, more than 80% of mobile data is consumed indoors already (NasrM. 2020). That is, the legacy Wi-Fi users and V2X users can coexist if the two systems are limited to operate indoor and outdoor, respectively. Moreover, exploiting the fact that such a setting is very likely in an urban scenario, we devote this research to analysis of fundamental problems induced in the setting. (Notice that in a suburban scenario, there will not be much of an inter- RAT interference issue as there will unlikely be other RATs' transmitters alongside the roads.) Overall, this assumption is expected to provide a conservative guideline since when the spread spectrum is adopted, the two RATs will be separated even better.

Second, the *vehicles' distribution* follows a Poisson point process (PPP). As shown in Figure 2, a generalized “square”-shaped space is assumed instead of an example road segment, for the most generic form of analysis as done in a related literature (KimS. 2019). The environment represented by the system space $\mathbb{R}^2_{\text{sys}}$, which is defined on a rectangular coordinate with the width and length of D m. Therein, a V2X network is defined as a homogeneous PPP, denoted by Φ_D, with the density of $\lambda(>0)$. The position of vehicle i is denoted by $\mathrm{x}_i = (x_i, y_i) \in \mathbb{R}^2_{\text{sys}}$. Note also that the PPP discussed in this research is a stationary point process where the density λ remains constant according to different points in $\mathbb{R}^2_{\text{sys}}$. It is important to note that based on the modeling with PPP, the uniformity property of a homogeneous point process can be held (Vere-JonesD. 2013). That is, if a homogeneous point process is defined on a real linear space, then it has the characteristic that the positions of these occurrences on the real line are uniformly distributed. Therefore, we can assume that the vehicles are uniformly randomly scattered on the road with different values of intensities and CW values, which will be provided in Section <Numerical Results>.

Regarding the PPP, it is important to notice that a PPP Φ is defined as a "marked" point process where the speed variance, Ψ, is associated with each point x_i. This mark is an independent normal random variable as seen from a point x_i. Specifically, let point process $\Phi = \{\mathrm{x}_i : i \in \mathbb{N}\}$ denote the locations of the nodes. Importantly, it is assumed that the mark of a point does not depend on the location of its corresponding point in the underlying (state) space.

Third, we assume *four possible results of a packet transmission* including successful delivery (SUC), packet expiration (EXP), and two types of collision: synchronized transmission (SYNC)

and hidden-node collision (HN) (DietrichS. 2018). A SUC is a case where a packet does not undergo contention nor collision. An EXP occurs when a packet has to be discarded while being backed off due to the channel being busy. A SYNC refers to a situation where more than one TX's start transmission at the same time. A HN is the other type of collision, which occurs due to a hidden node.

Fourth, we consider a *BSM broadcast* in a single, 10-MHz channel. The analysis framework and result that will be presented throughout this research are based on assumptions of: (i) broadcast of BSMs and (ii) usage of a single channel only. It means that the result has a room for improvement if a multi-channel operation is adopted. As such, the results that will be demonstrated in Section <Numerical Results> can be regarded as the worst-case, most conservative ones.

Fifth, the *speed of each vehicle* is characterized as a random variable. Speeds are selected by the driver. Different drivers select different speeds, dependent upon many variables (vehicle limitations, roadway conditions, driver ability, etc.). No single speed value can accurately represent all the speeds at a certain location. A speed distribution provides that information. Operating speeds have been found to be normally distributed (USDOT, Speed concepts: Informational guide 2009). This is fortunate since using that premise (probability is normally distributed) allows for some straightforward calculations.

Analysis Part I: Interference between V2X and Wi-Fi

Notice that we adopt aggregate interference as the metric for evaluation of the inter-RAT interference. The rationale is that a V2X network is very dynamic. As such, it is less practical if

we focus on a certain vehicle to measure the interference since it will not represent the entire network stably enough. Let $\mathbf{I}_{\mathrm{agg},j}$ denote an instantaneous aggregate interference measured at the *j*th node of a RAT from the other RAT, which is formally written by

$$\mathbf{I}_{\mathrm{agg},j}(\mathrm{x}_t, \mathrm{x}_r) = \sum_{j \in \mathcal{S}_t} \frac{\mathrm{P}_t \mathrm{G}_t(\mathrm{x}_t, \mathrm{x}_r) \mathrm{G}_r(\mathrm{x}_t, \mathrm{x}_r)}{\mathrm{PL}(\mathrm{x}_t, \mathrm{x}_r)}$$

where the variables are given as follows: $\mathbb{R}^2_{(\cdot)}$ denotes the twodimensional space where RAT $(\cdot)$ is defined; $\mathrm{x}_{(\cdot)} = (x, y)$ where $x, y \in \mathbb{R}^2_{(\cdot)}$ gives the position of a station (STA) belonging to the RAT $(\cdot)$; $\mathcal{S}_t$ defines the set of STAs belonging to the interfering RAT; P_t denotes the transmit power of the interfering STA; G_t and G_r give the antenna gain of the interfering STA and the victim STA, respectively.

Also notice that the path loss can be formulated as

$$\mathrm{PL}(\mathrm{x_t}, \mathrm{x_r}) = \mathrm{PL_{int}} + \mathrm{PL_{ext}}\ [\mathrm{dB}]$$

As shown above, path loss is divided into two components. First, the path loss within the same system is written as

$$\mathrm{PL_{int}}(\mathrm{x}_t, \mathrm{x}_r) = 10 \log_{10} \|\mathrm{x}_t - \mathrm{x}_r\|^{\alpha}.$$

The other component is the path loss between the dissimilar systems, which is given by (3GPP, 5G; Study on channel model for frequencies from 0.5 to 100 GHz 2022)

$$\mathrm{PL_{ext}}(\mathrm{x}_t, \mathrm{x}_r) = \mathrm{PL_{int}}(\mathrm{x}_t, \mathrm{x}_r) + \mathrm{PL_{tw}} + \mathrm{PL_{in}} + \mathbb{N}(0, \sigma^2)$$

where the path loss through the wall (i.e., O2I) is characterized as

$$\mathrm{PL_{tw}} = \mathrm{PL_{npi}} - 10 \log_{10} \sum_{i=1}^{N} \left(p_i 10^{-L_{\mathrm{mat},i}/10} \right)$$

with $L_{\mathrm{mat},i}$ indicating the penetration loss of the material i and p_i is the proportion of the material i. Also, $\mathrm{PL_{in}}$ gives the indoor loss, which is a function of the distance between the indoor STA and the wall.

We translate the interference power into the interference-to-noise ratio (INR), which is given by

$$\mathrm{INR}(\mathrm{x}_t, \mathrm{x}_r) = \frac{\mathbf{I}_{\mathrm{agg},j}(\mathrm{x}_t, \mathrm{x}_r)}{\mathrm{N}}$$

where N gives the noise power. The display in the INR is to understand the interference power in reference to a characteristic that is singular to the particular RAT, i.e., the noise power.

Analysis Part II: Proposition of V2X Load Lightening Protocol

Now, we proceed to technical details of this research's proposition of *prioritizing the V2X networking according to the accident risk.*

Quantification of Accident Risk

We start by identifying the accident risk metric. We choose the variation of speed, denoted by Ψ, as the key indicator of the driving risk to a vehicle is exposed while driving:

$$\Psi = \sqrt{(v - \mathrm{v}_L)^2}$$

where v_L gives the speed limit of the road.

In fact, speed has been found as the most direct indicator of the risk of an accident (W. MandaS. 2019). This research assumes that each vehicle moves at speed of v meters per second (m/s), which is a varied factor as shall be shown in Section <Numerical Results>. The direction of a

vehicle follows a uniform distribution in the range of $[0,2\pi]$. A node is bounced off when reaching at the end of $\mathbb{R}^2$ in order to stay in the space, which hence keeps the total intensity the same. As such, the proposed protocol allocates the backoff counter according to the quantity of Ψ.

We use the variance of speed from the speed limit of the road as the metric measuring the driving risk. The rationale behind this is the "easiness" in getting a speed limit. For instance, a speed limit is an easy number to obtain in many commercial Global Positioning System (GPS) applications (e.g., Google Maps). Reliance on such an easily available quantity increases the applicability of the proposed algorithm. It can be replaced with other relevant parameters: e.g., the mean speed over the neighboring vehicles.

We wanted a more aggressive scheme to benefit "dangerous" vehicles than allocating a higher access category (AC) in EDCA. In essence, the performance of EDCA still depends on CW, which may be hazardous for a very urgent safety-related packet delivery.

We remind that the key metric in the proposed protocol is Ψ that was presented earlier in this subsection. The main idea of the proposed protocol is to divide the distribution of Ψ into multiple discrete sections and apply different backoff allocation patterns.

Given that, we can start formulating the distribution of Ψ. We found the probability distribution function (PDF). As shown in Figure 3, the speed's variance, Ψ, is found to follow a Gamma distribution with the shape parameter of $1/2$ and the scale parameter of $2\sigma^2$:

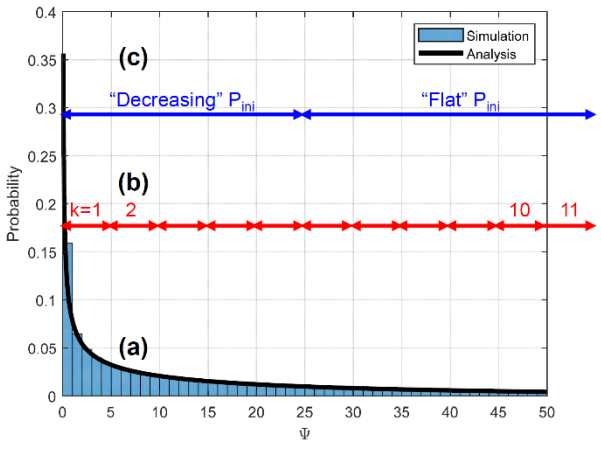

Figure 3. Graph. PDF of Ψ (with $X \sim N(60, 25)$): (a) Model validation between simulation and analysis of $f_\Psi(\psi)$; (b) Categorization of Ψ (with K = 11 and Q = 5); and (c) An example allocation of backoff values for the proposed protocol

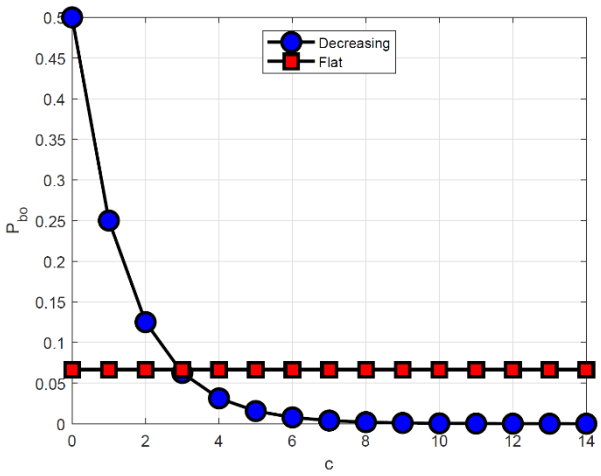

Figure 4. Graph. Backoff probabilities versus the value of backoff counter, illustrating the difference in decrementing the backoff counter between decreasing and flat backoff mechanisms

$$f_\Psi(\psi) = \frac{1}{\Gamma(1/2)\sqrt{2}\sigma}\psi^{-\frac{1}{2}}e^{-\frac{\psi}{2\sigma^2}}, \quad \psi \geq 0.$$

Now, as a means to characterize the driving risk, we categorize the metric, Ψ, into a number of regions on its PDF. The reason for this categorization is, as seen from Figure 3, the PDF of Ψ is openended to the right (positive side); hence, a value of Ψ itself is not appropriate to be used in categorization.

Note that two key parameters are defined to identify a categorization: (i) the number of categories, K, and (ii) the step size, Q. The range of Ψ for each category, k, is given by

$$(k-1)Q \leq \Psi \leq kQ$$

which, in turn, gives k as a function of Ψ as

$$k = f(\Psi) = \left[\frac{\Psi}{Q}, \frac{\Psi - 1}{Q} + 1\right], k \in \mathbb{Z}.$$

During a backoff process for a BSM that is shown in Figure 4, the value of k is assumed to be fixed; in other words, a vehicle does not experience a change of Ψ greater than Q. We assume 10 Hz of the BSM generation frequency--i.e., 10 BSMs per second, which leads to 100 msec per BSM. Notice that a 100 msec is a short time in relation to the reality on the road--i.e., for a vehicle to experience a change in Ψ. Moreover, even if so, as an IEEE 802.11-based system, the V2X is supposed to support such a situation at "best effort."

Proposed Protocol

Now, we propose a protocol that allocates $P_{\text{bo}}(c) := \text{P}[\text{backoff} = c]$ based on the categorization of Ψ into k. More specifically, with a value of k being larger than $\left\lceil\frac{K}{2}\right\rceil$ (i.e., the area of "large" Ψ's, which indicates cases of greater deviations in a vehicle's speed), we allocate backoff counters in a "decreasing" pattern. In contrast, for k being smaller than $\left\lceil\frac{K}{2}\right\rceil$ (i.e., the area of "small" Ψ's, which means cases of smaller deviations in a vehicle's speed), the backoff counters are allocated in a traditional "flat" fashion in which the probability of any backoff counter value is equal.

Figure 4 demonstrates an example with $K = 11$ and $Q = 5$. On the PDF, it indicates the principle of the proposed protocol: a larger value of $k \in \{1, 2, \cdots, K\}$ (which occurs with a smaller probability, $f_S(s)$) takes a smaller backoff value with a higher probability.

The proposed protocol can be interpreted as follows. In a “decreasing” backoff allocation, a node is given a higher probability for a smaller backoff value, which increases the chance of winning the medium. A “flat” pattern indicates backoff allocation in a uniform distribution, which is currently adopted by the IEEE 802.11 (Kim and Bennis, Spatiotemporal analysis on broadcast performance of DSRC with external interference in 5.9 GHz band 2019).

We claim that the key benefit of the proposed protocol is modification of the CSMA that is adopted in IEEE 802.11. As such, it will achieve a higher backward compatibility and therefore an easier adoption in practice.

Numerical Results

Interference Measurement: V2X-to-Wi-Fi vs. Wi-Fi-to-V2X

The first metric to display the interference is the *aggregate interference power*, which was quantified as $\mathbf{I}_{agg}$ in Section <Analysis Part I: Interference between V2X and Wi-Fi>. Specifically, Figure 5 presents the aggregate V2W and W2V interference, respectively. We highlighted that the interference power needs to be compared to a reference to assess its impact to the victim RAT. Thus, we refer $\mathbf{I}_{agg}$ to the RX sensitivity of the victim system. It enables us to quantify how severe the interference affects a RX of the victim RAT by being "sensed," and hence corrupting its desired signals.

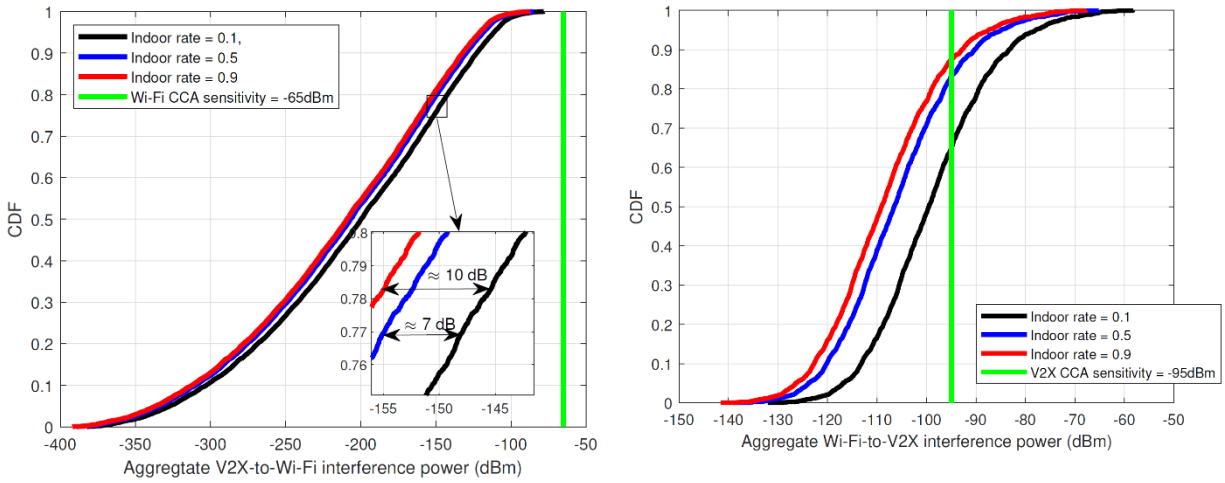

(a) V2X to Wi-Fi (b) Wi-Fi to V2X

Figure 5. Graphs. Aggregate inter-RAT interference according to the Wi- Fi's indoor deployment rate (with 64-QAM, Coding rate = 3/4)

Furthermore, each curve in Figures 5a and 5b represents an indoor rate of {0.1, 0.5, 0.9}. (Recall that the indoor rate means the rate of indoor deployment of Wi-Fi TX devices. We also remind that the assumption is rooted on the fact that more than 80% of mobile data is consumed indoor (NasrM. 2020).) Figure 5a shows that {0.5, 0.9} of indoor rates lead to {7, 10}-dB increase in the interference power. However, all the cases remain below the clear channel assessment (CCA) sensitivity of the victim RAT (i.e., Wi-Fi), which implies that the V2W interference causes no harm on the Wi-Fi's operation regardless of the Wi-Fi's indoor rate.

In stark contrast, according to Figure 5b, the W2V interference is quite more significant. It is an interesting finding because the O2I loss is supposed to apply the same in both directions of V2W and W2V. This asymmetry in the aggregate interference comes from the key difference in the radiation type at a TX antenna. That is, it is likely that a vehicle has an omnidirectional antenna because the main pursuit of safety-critical V2X communications is to broadcast safety messages

to as many vehicles as possible around the vehicle. In contrast, a Wi-Fi TX employs a more highly directional antenna as a means to accomplish a higher data rate.

We also evaluated the interference in terms of the *INR*, which was defined in Section <Analysis Part I: Interference between V2X and Wi-Fi>. Figure 6 shows the distribution of the INR with the Wi-Fi's indoor deployment rate of 0.9. Different curves represent different densities of V2X and Wi-Fi: , $\lambda_c > \lambda_w$: $(\lambda_c, \lambda_w) = (500, 200)/\text{km}^{-1}$, $\lambda_c = \lambda_w$: $(\lambda_c, \lambda_w) = (200, 200)/\text{km}^{-1}$, and $\lambda_c < \lambda_w$: $(\lambda_c, \lambda_w) = (200{,}500)/\text{km}^{-1}$.

We compared the INRs to thresholds of -6 and 0 dB of INR (S. KimE. 2017). It is noteworthy that we chose conservative values for the INR threshold, which are referred from 5G terminal receivers usually adopting higher digital modulation indexes than V2X and Wi-Fi. Moreover, notice that we assume the indoor rate of 0.9. Given that as much as 80% of Wi-Fi users are usually placed indoor (NasrM. 2020), an even higher proportion of Wi-Fi users will likely be deployed indoor in an environment where the node density is high, such as an urban area.

Figure 6a shows that approximately 60% of the vehicles contribute to interference into the Wi-Fi users, commonly for all the three density scenarios. However, as shown in Figure 6b, the chance is far higher for Wi-Fi users to cause interference exceeding the INR thresholds. Specifically, the likelihood that the W2V interference exceeds the thresholds is nearly 100%. The reason for this asymmetry between the V2W and W2V interference has already been discussed: the Wi-Fi users employ an antenna with a higher directivity than the V2X users do.

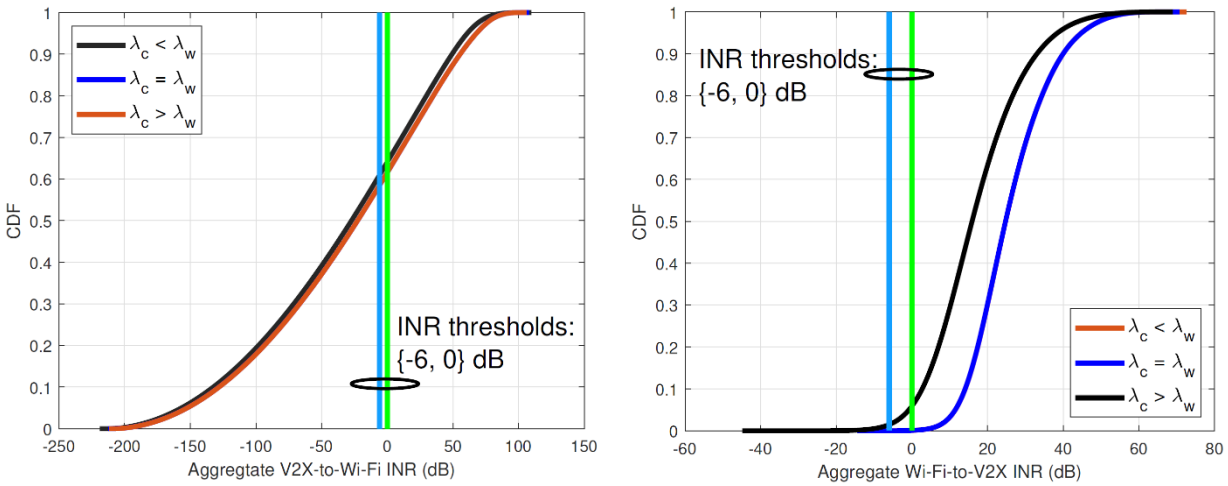

(a) V2X to Wi-Fi (b) Wi-Fi to V2X

Figure 6. Graphs. Aggregate INR according to the density of V2X and Wi-Fi (Wi-Fi's indoor deployment rate of 0.9, 64-QAM, Coding rate = 3/4)

The overall observation from Figures 5 and 6 is that the V2X is the victim at large. It suggests that under the Wi-Fi-V2X coexistence, the Wi-Fi can still achieve its target signal reception level even with the current multiple access methodology. However, the same is not true for the V2X: a modification on the current multiple access method is urgently needed to deal with the interference in order to survive in the coexistence. That rationalizes this research investigating how to optimize the traffic load of a V2X network according to the danger level, whose results will follow in the next subsection.

Performance of Proposed Access Mechanism

This subsection displays how effective our proposed mechanism is in lightening the load of a V2X network. Recall from Section VI the three metrics that this research adopts: Figures 7 through 9 presents the probability of a successful packet transmission (τ), the probability of packet collision over the air (P_b), and PDR, respectively. In the three figures: (i) a solid line

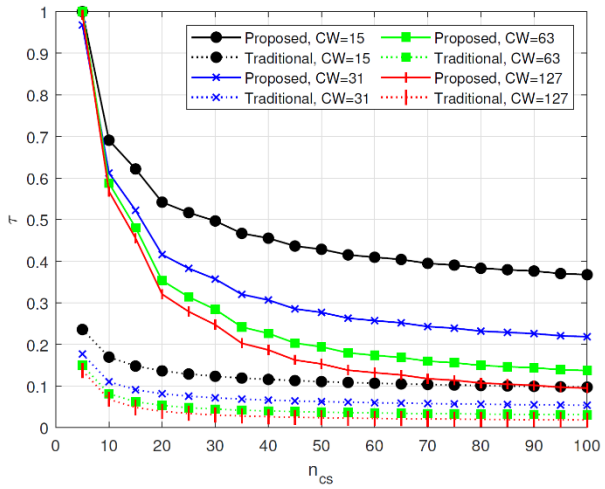

Figure 7. Graph. Transmission probability versus number of competing vehicles

represents the proposed mechanism, while a dotted line constitutes the traditional CSMA/CA (J. W. TantraC. 2005); (ii) different colors indicate different CW values.

Figure 7 shows the probability that a vehicle has been able to go through a backoff process and transmit a BSM, denoted by τ, versus the number of vehicles within its carrier sense range, n_{cs}.

Commonly for all the CW values, the τ decreases with an increased n_{cs}. This tendency is attributed to P_b being kept relatively low at all n_{cs}. (Although we do not present a separate result for P_b, our study suggested an approximately 15% even with 500 competing nodes within one's carrier-sense range.) The reason is the small value for τ as shown in Figure 7, which is plausible because a beaconing period contains a very large number of slots--i.e., the length of a beacon is as large as 750, based on an assumption of 66.7 μsec for a slot time and 50 msec for a beaconing period.

Also, the results are intuitive: P_b is increased with a greater n_{cs}. One can observe that a smaller value of r yields a lower P_b (which, in turn, leads to a higher Pstart as such). The rationale behind this result is that a smaller r serves as a more drastic decrement of the backoff probability.

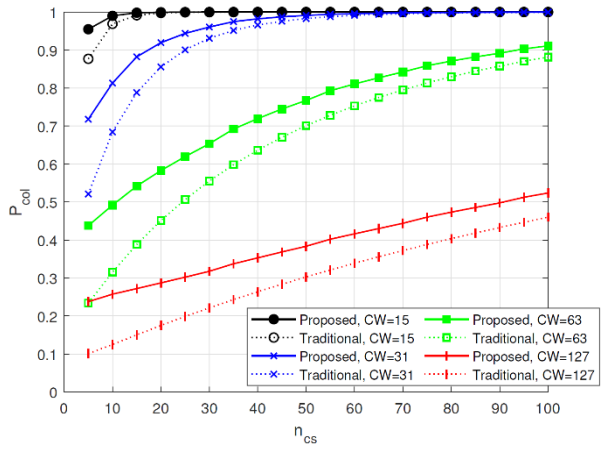

Figure 8. Graph. Collision probability versus number of competing vehicles

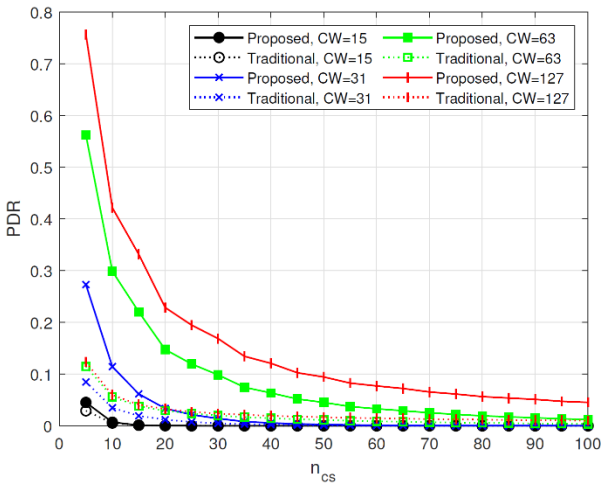

Figure 9. Graph. PDR versus number of competing vehicles

Figure 8 presents the probability of a collision, P_{col}, versus n_{cs} according to CW. One can easily find from Figure 8 that a larger CW yields a lower P_{col}.

Recall that the P_{col} is dominated by collisions (viz., SYNC and HN), both of which are functions of τ measured at each vehicle. There are several important points to discuss about the SYNC and HN: (i) a larger CW is effective in alleviating both SYNC and HN, and therefore P_{col} as a direct consequence; (ii) For a CW, HNs occurs more often than SYNCs. The reasoning is that the number of hidden terminals is larger than that of STAs causing a SYNC since the area of HN is larger than that of SYNC (Kim and Bennis, Spatiotemporal analysis on broadcast performance of DSRC with external interference in 5.9 GHz band 2019); (iii) the proposed protocol yields a higher P_{col} than the traditional CSMA/CA since, on average, it allows certain nodes more likely to transmit.

Figure 9 shows PDR versus n_{cs}. We note the following key observations. First, the proposed protocol yields a higher PDR while it showed an unfavorable P_{col}, due to a higher margin in τ. Second, the margin that the proposed protocol yields in PDR gets increased with a larger CW. The reason is that P_{col} gets very small (i.e., ≈ 0) with a larger CW such as 511.

The proposed scheme yields a higher PDR compared to the proposed mechanism as shown in Figure 9, despite a higher P_{col} as found in Figure 8. The reasoning behind this phenomenon is attributed to a higher τ as Figure 7 presents. The predominance of CW in determination of PDR suggests that P_{col} acts as the most critical factor in inducing the two quantities. As observed in Figure 8, a larger CW yields a lower P_{col} and broadens the outperformance of the proposed scheme over the proposed one. Henceforth, all these results suggest that a V2X network can actively increases CW as an effort to combat a lower PDR as a result of high road traffic, i.e., a large n_{cs}.

Chapter 3. Task 2: DSRC in 4.9 GHz Public Safety Band

This task is dedicated to studying the feasibility of sharing the 4.9 GHz public safety band between the incumbent systems and V2X users. We study the problem of sharing the 4.9 GHz band between the incumbent systems and V2X users. The findings reveal that spectrum sharing can be achieved in a space-division manner. Specifically, the usability by V2X users is determined by the incumbent RX location. In a highly populated area, a directional antenna can improve the possibility of sharing the spectrum between the two systems.

Background

Legislative Background

The 4.94-4.99 GHz spectrum (also referred to as the "4.9 GHz band") plays a crucial role in ensuring the effective communication and coordination of public safety and emergency response entities. This spectrum, allocated specifically for public safety use, provides a dedicated and secure channel for first responders, law enforcement agencies, fire departments, and other emergency services to communicate seamlessly during critical situations.

In 2002, the U.S. FCC designated the 50-MHz spectrum for the use of public safety purposes. According to the current band plan the band is divided into ten 1 MHz channels and eight 5 MHz channels, while limiting channel aggregation bandwidth to 20 MHz. Although nearly a hundred thousand entities are eligible to be licensed, only around three thousand licenses have been granted by the FCC. The FCC expressed concern that the spectrum has not reached its full

potential and thus seeks other options to make this spectrum utilized and gain its maximum efficiency.

In September 2020, the FCC voted on the licensing of making the 4.9 GHz widely available for commercial use and allowing leases to third parties, making the spectrum reach its true potential. However, in the summer of 2021 the new administration at FCC halted the process of leasing the spectrum stating that the spectrum shall only be used for the purpose of public safety.

The Code of Federal Regulation (CFR) section 90.523 (90.523CFR 2023) defines the eligibility of parties to hold the license for the spectrum, elaborating that all local and state governmental entities are eligible to hold a 4.9 GHz spectrum license, limiting the federal government to not hold the license but allowing them to share it among local and state safety systems.
The sharing of the systems must be drafted in the form of a legal biding document, explaining in detail the use of the spectrum towards public safety, protection of the lives of citizens, their health or property.

A *band plan* is described as the division of the plan to avoid interference among channels operating in adjacent zones. As per CFR section 90.1213 (90.1213CFR 2023), the 4.9 GHz spectrum is permitted to be aggregated among channels comprising of five different bandwidths 5, 10, 15, and 20 MHz. The maximum bandwidth of a channel that could be allocated to a system in 4.9 GHz system is 20 MHz.

Channels starting from 4940.5 MHz to 4944.5 MHz are 1 MHz allowed bandwidth channels, followed by eight 5-MHz channels up till frequency band 4982.5 MHz, from 4985.5 MHz to 4989.5 MHz are 1-MHz channels as well.

Technical Background

To maximize the spectral efficiency of the communication over a designated channel the FCC defines spectral emission masks (SEMs). In CFR section 90.210 (90.210CFR 2023), the devices that are being deployed in 4.9 GHz spectrum are required to be in compliance with the FCC-defined masks commonly known as the DSRC-A mask, and the DSRC-C mask. In Figure 10, a comparison of existing masks (O'HaraS. 2000) versus the FCC standards is shown along with the attenuation in decibels.

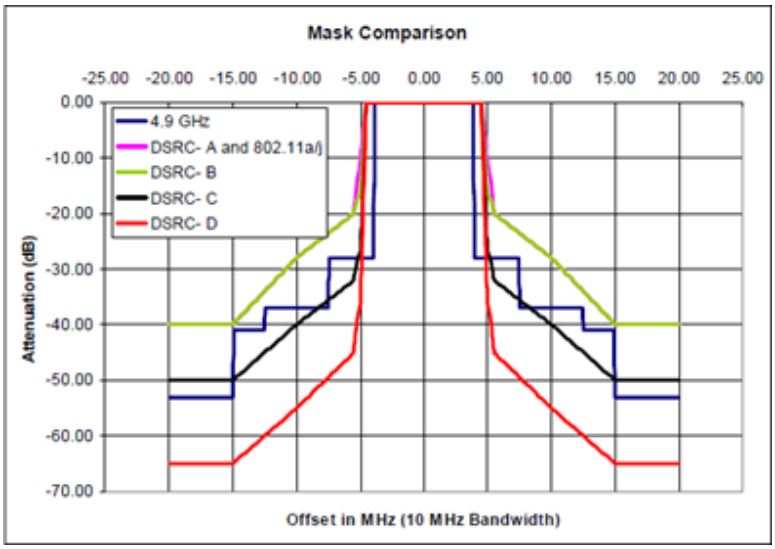

Figure 10. Graph. Regulation on the 4.9 GHz mask in comparison to related standards

According to CFR section 90.1215 (90.1215CFR 2023), the transmitting power of stations operational in the spectrum of 4.940 to 4.990 GHz must not exceed the maximum limits. Table 1 lists the low-power and high-power maximum conducted power for the aggregated bandwidth of the channels in the safety band spectrum.

Table 1. Power limits for channel bandwidth of 1-20 MHz in 4.9 GHz spectrum

Bandwidth (MHz)	Low-power max (W)	High-power max(W)
1	0.005	0.1
5	0.025	0.5
10	0.050	1.0
15	0.075	1.5
20	0.100	2.0

Spectrum Sharing in 4.9 GHz Band

In consideration of underutilization of the band (USFCC 2021), we propose that the 4.9 GHz band accommodates V2X communications as a *secondary system*. The International Telecommunication Union (ITU) designates allocations as 'primary' when the service has priority use of the band (this is co-primary where there are several services) or 'secondary' when the service may operate as long as it does not interfere with 'primary' services. In the following subsections, we identify technical details for (i) the incumbent systems of the band and (ii) spectrum sharing methods of operating V2X communications as a secondary system in the band.

Incumbent Systems in the 4.9 GHz Band

The incumbent and neighboring systems can be found from the relevant federal regulatory documents such as the Title 47, Part 2 of CFR (IA2CFR 2023) and the U.S. spectrum allocation map (NTIAUS 2023). In particular, near the 4.9 GHz band, several systems hold an exclusive right for operation--viz., U.S. Navy, radio astronomy, etc.

Initially, the 4.9 GHz spectrum was allocated to the federal government by the U. S. FCC. However, after 1999, the upper half of this spectrum was reallocated for non-governmental

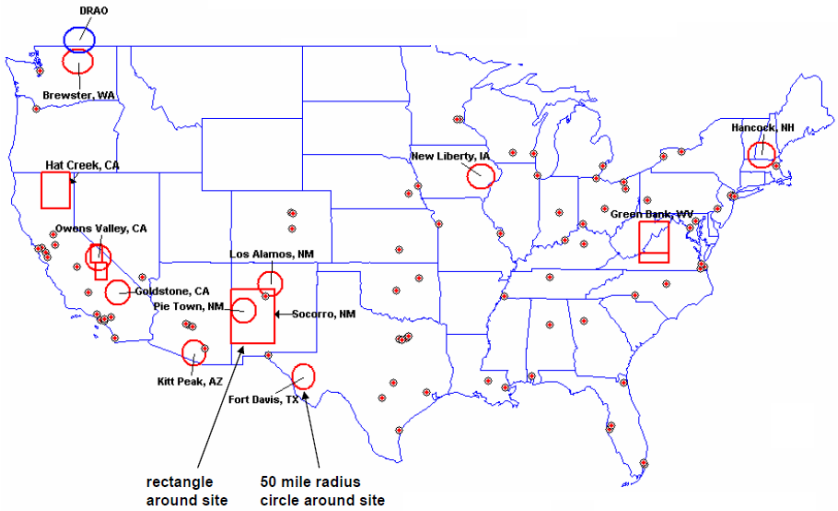

Figure 11. Map. Radio astronomy sites in the U.S. (B. RinehartD. 2010)

public safety services. Nevertheless, the lower region of 4.9 GHz spectrum is still used by the U.S. Navy as they conduct the Cooperative Engagement Capabilities (CEC) training. If licenses are to be leased in the lower half of the 4.9 GHz band, they are bound to receive some airborne interference in the areas of operational high power U.S. Navy base stations or in certain situations even 250 miles away from the transmitting towers.

Therefore, any organization who wants a license for airborne operation in the 4.9 GHz band should file a waiver request, where they could send an application to allow them the use of 4.9 GHz band and modify their operations aligning it with the code defined by the U.S. Navy.

According to the U.S. frequency allocation (NTIAUS 2023), the *radio astronomy* is operating in the 4.990 to 5.000 GHz band on primary basis and operating on 14 specific locations on secondary basis within the range 4.950-4.990 GHz.

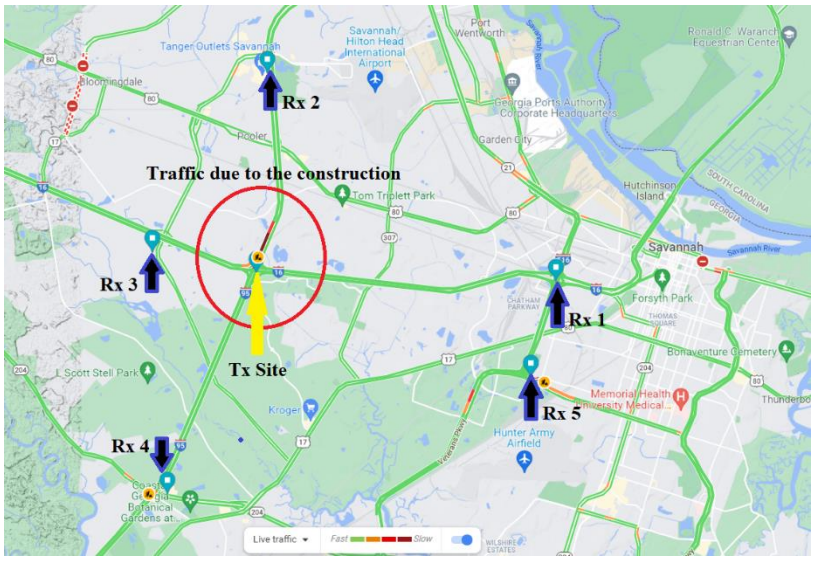

Figure 12. Map. TX site and location of RXs along with live traffic

Entities leasing the 4.9 GHz are required to operate closely to the ground leaving the operations of radio astronomy without any interference. The same reason goes along with the prohibition of any airborne use of the 4.9 GHz band.

In Figure 11, all the radio astronomy sites are shown along with the operational base information in cities around the U.S.

Method of Sharing the 4.9 GHz Band with V2X

The U.S. has been experiencing increases in roadway deaths since 2015 (NHTSA, NHTSA Estimates Traffic Fatalities Continued to Decline in the First Half of 2023 2023). Interstate 16 (I-16) is not exempt from this crash and fatality experience (WTOC 2021). Ongoing construction adds to the challenges experienced by motorists. Considering the aforementioned spectrum sharing setting, establishing a transmitter station (TX) along the ramp that could help the inbound and outbound traffic with real-time information regarding major accidents or updates along the route of the interchange.

There were two main reasons for choosing the interchange as the TX location. Firstly, the nearest radio astronomy site is located in Atlanta, Georgia, which is more than 250 miles from the prime location. Secondly, the position of the interchange will serve as a beacon to the traffic for the Savannah airport, downtown Savannah, and inbound traffic from I-16 East to Tybee Island and Hilton Head Island. Furthermore, 5 locations for stationary RXs are selected around the TX, which are displayed in Figure 12. Also notice in the figure that live traffic can also be seen highlighted with a red circle.

Simulation Results

Setup and Parameters

Table 1. Key parameters for simulation

Parameter	Value
Radio access	Long-Term Evolution (LTE)
Carrier frequency	4.9 GHz
Bandwidth	10 MHz
Path loss model	Free space path loss (i.e., LoS)
TX antenna height	{60, 2} m
TX power	1 W (30 dBm)
RX sensitivity	-85 dBm

Key parameters for the simulations are summarized in Table 2. By defining the TX frequency as 4.98 GHz and limiting the power of the TX to 2 Watts (W) maximum allowed by FCC CFR section 90.1215 (90.1215CFR 2023).

Communication links will be plotted using the link function along with the ideal coverage of the TX site. All RXs should fall ideally inside the borders of the ideal coverage network. Another

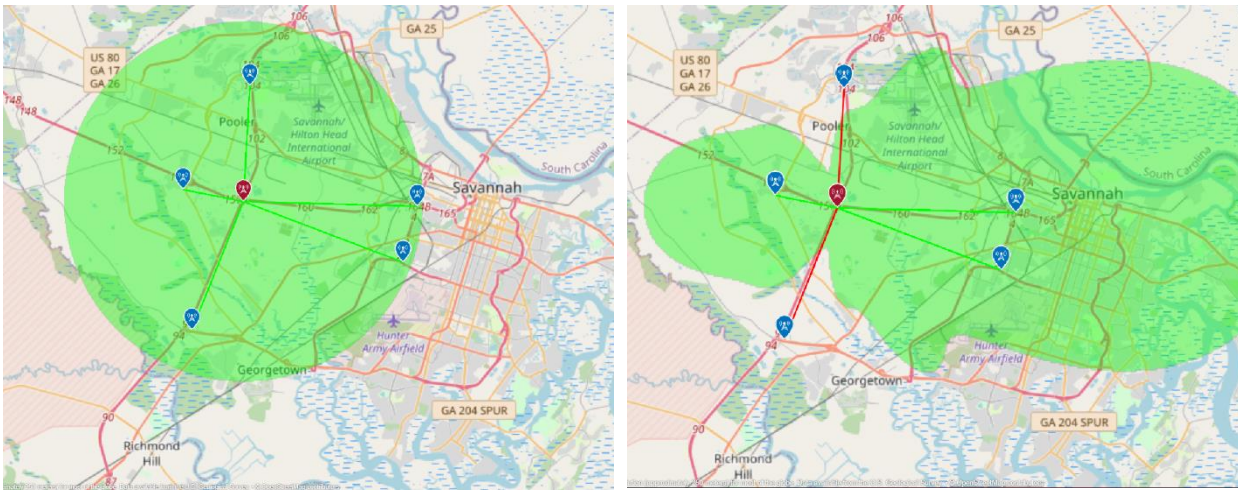

(a) Dipole antenna (b) Directional antenna

Figure 13. Map. Comparison of V2X service coverage according to antenna type at TX (with TX height of 60 m)

useful function used in the simulation is the rain propagation model, which was used to represent the weather condition for the sites.

The central point of this simulation study is a comparison of the antenna radiation types--viz., dipole and directional antennas. The next topic of discussion is the feasibility of spectrum sharing between the incumbent systems and V2X in the 4.9 GHz band.

Results and Discussion

Figures 13 and 14 compare the coverage of a V2X system near the area of Savannah, Georgia. Notice that subfigures (a) and (b) represent a TX adopting a dipole and a directional antenna, respectively.

(a) Dipole antenna (b) Directional antenna

Figure 14. Map. Comparison of V2X service coverage according to antenna type at TX (with TX height of 2 m)

In Figure 13a, it can be viewed that all the RX sites are falling under the umbrella of the TX site, implying that the simulation received total coverage even when rain possibilities were applied. However, if our receivers (RXs) were nearer the downtown Savannah area it would have been inefficient and the coverage at their end would have outage.

This changes in Figure 13b. With a directional antenna, RX 2 and RX 4 fell out of the coverage. However, the better thing about this antenna is the wide coverage of the directional in the downtown Savannah region. If the project is to be more focused towards a plan that can be deployed in the downtown Savannah region, then it could be more useful.

While a cell tower can easily be as high as 60 m, a lower TX height makes better sense if a vehicle-to-vehicle, distributed environment is preferred. Then the concern is a significant reduction in the coverage. As such, we assumed that the TX antenna is placed closer to downtown Savannah where higher traffic is observed. Figure 14 illustrates this change. In fact, the Savannah metro area is experiencing increasing vehicular congestion (GDOT 2021). Further, 65% of the mentioned traffic was falling in the downtown Savannah area with the directional

antenna as displayed in Figure 14, the simulation is covering from Liberty Parkway Street to Savannah State University a distance of 5 miles. Catering to the traffic of the university student's vehicle and tourists, it seems to be ideal to implement a TX away from the incumbent systems existing in the 4.9 GHz spectrum.

Practical Implications

In the models that have been presented in this section, a TX gave roughly an approximate 5-mile radius of cell coverage. This approximation was made using a moderate size antenna that could easily be deployed along with traffic signals. Predicated on this assumption, around 300,000 residents of Savannah city (LLCMacrotrends 2021) can benefit besides the tourists traveling around Savannah River and nearby beaches.

The spectrum sharing model is designed to maximize the connection among vehicles near the downtown Savannah region and the Savannah/Hilton Head International Airport, which likely are the most populated areas. Based on the spatial separation displayed in Figures 13 and 14, we propose that spectrum access can be given to the IoT systems unless they cause less interference than allowed by the incumbent systems' interference requirement.

We also claim that this model can be altered further by cascading several TX sites throughout the downtown and neighboring suburbs of Savannah, keeping the system operational along with other incumbent systems lying in the 4.9 GHz spectrum.

Chapter 4. Task 3: Transition to C-V2X

This task was focused on analyzing the technical impacts of the transition from DSRC to C-V2X in the spectrum of 5.895-5.925 GHz, compliant with the recent regulatory change.

An important thing to notice is that the contents of this task many parts in common with Task 4; as a result, the information required to comprehend the content of this task can also be located in Section <Task 4: 30 MHz Application Map>.

Background

Motivation

C-V2X has been designated as the sole technology implementing the ITS applications in the 5.9 GHz band. It requires the existing DSRC licenses to transition to C-V2X.

Proposed Scope of Work

Recognizing the need to transition from DSRC to C-V2X, this research lays out foundational research aiming to address the following technical problems.

First, it builds geographic and channel models. The 3GPP TR 36.885 (3GPP, Study on LTE-based V2X Services; (Release 14) 2016) will be referred to for the establishment of models for (i) the deployment of vehicles and RSUs, (ii) vehicle density and speed, and (iii) path loss and spatiotemporal channel effects, viz., shadowing, Doppler effect, etc.

Second, it delves into ITS messaging methods that C-V2X supports. It is anticipated that the ITS messaging system can work to prioritize and deliver messages more efficiently in the upper 30 MHz, such as by adjusting message timing to provide multiple types of messages on a single channel to provide the same level of safety to vehicles as can be done on the existing spectrum. This project inspects the feasibility of such messaging methods in a C-V2X system.

Third, it investigates advantages that C-V2X poses over DSRC. In the Rules and Regulations, the FCC has identified several technical advantages of C-V2X over DSRC. This project provides an analysis framework to confirm the advantages, which include but are not limited to:

- C–V2X functionality can offload less time-critical V2X communications to the cellular network, thereby supporting safety-critical communications
- C–V2X is better for achieving network effects insofar as cost efficiencies support deployment on a more accelerated basis
- C–V2X technology can leverage cellular networks and thereby reduce the infrastructure cost associated with deploying V2X communications
- Because C-V2X operates on both 20- and 10-MHz channels, it could support throughput throughout the 30 MHz of spectrum that would be available.

As an effort to address these problems, this research put extensive effort in designing a computer simulator, in-lab testing suite, and a field-test apparatus. Technical details will follow in Sections <Simulator Development> through <In-Lab Testing Development>.

Simulator Development

This part of the research is dedicated to development of a comprehensive computer simulation framework that features “vertical integration” throughout geographic/traffic setup and PHY/RRC-layers of C-V2X. The highlight of the contribution is the implementation of modulation and coding scheme (MCS), which completes a holistic view on the performance of a C-V2X network depending on the geographic/traffic.

System Model

We notice that the system model that is used in this section will also form the basis of one that shall be used in this research. Readers should be aware of the similarity between the system models in the two sections.

A two-dimensional urban scenario (SAE, LTE-V2X deployment profiles and radio parameters for single radio channel multi-service coexistence 2022) with dimensions of 240 m × 520 m was established in MATLAB. The setup consists of three two-way road segments, with two junctions each comprising an RSU with a range of 150 m and utilizing a 20 MHz bandwidth. Each of the road segments is divided into two directions and each direction consists of two lanes. A total of six directions are considered: South-North, North-South, East-West 1, West-East 1, East-West 2, and West-East 2. Two parameters, λ and θ, correspondingly indicate the densities of vehicles and trucks, which are deployed randomly.

The trucks act as physical obstacles blocking V2X connections. The simulator features the ability to visually distinguish connected and blocked links between the RSU and neighboring vehicles. The blocked links are contributed by two types of physical obstacles: buildings and trucks, which can significantly attenuate the signals transmitted from the RSU to the neighboring vehicles.

The 3rd Generation Partnership Project (3GPP) Release 15 Long Term Evolution (LTE)-V2X for the physical-layer (PHY) (3GPP, 5G; Study on channel model for frequencies from 0.5 to 100 GHz 2022) and radio resource control (RRC) functions (3GPP, LTE; Evolved Universal Terrestrial Radio Access (E-UTRA); User equipment (UE) radio transmission and reception 2023) have been adopted in the LTE-V2X simulator using MATLAB. The sensing-based semi-persistent scheduling (SPS) algorithm for mode 4 has been employed, where the resource reservation interval (RRI) is set to 100 msec, and a random resource reselection counter (RC) between 5 and 15 is assigned to each vehicle.

The RC is decremented by 1 after each transmission, and once the RC reaches zero, the vehicle opts for new resources. A 20-MHz channel is divided into subchannels in the frequency domain and subframes in the time domain. Subchannels are further divided into resource blocks (RBs), each 180 kHz, and subframes into slots, each of which is 0.5 msec. The number of RBs per subchannel is variable depending on the MCS index. The Urban Micro (UMi)- Street Canyon path loss model has been incorporated in the simulation, considering the city road environment.

The number of allowed retransmissions for mode 4 sidelink is 1, and the number of subchannels per slot can vary from 1 to 10 (A. BazziG. 2019). A congestion control mechanism is integrated,

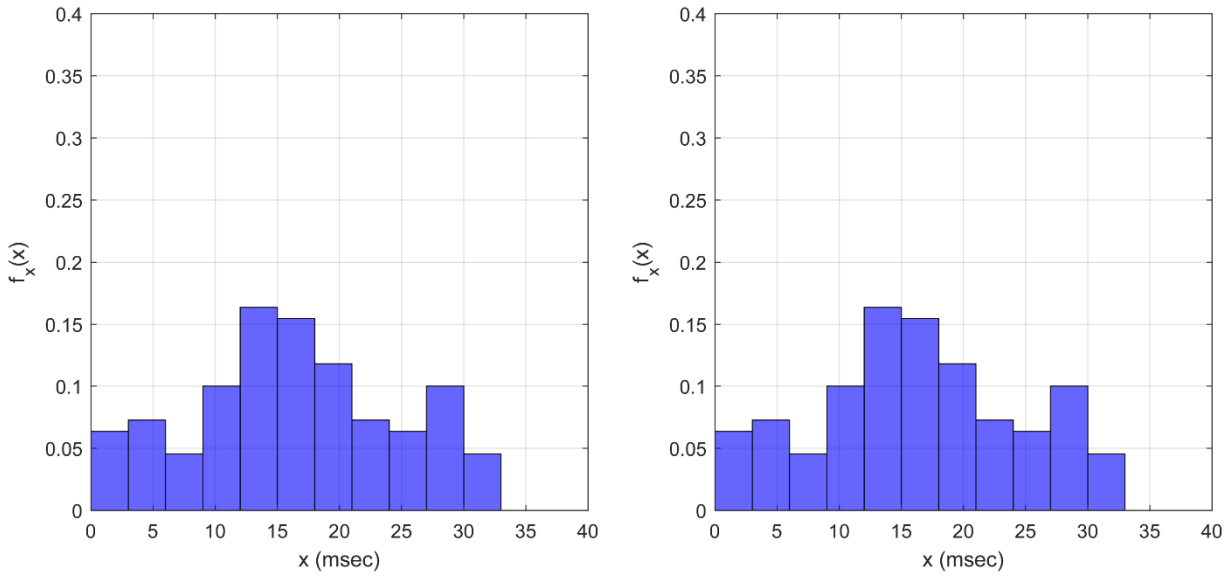

(a) MCS index = 7 (b) MCS index = 11

Figure 15. Graph. PDF of latency

where the channel busy ratio (CBR) and channel occupancy ratio (CR) are calculated. When the calculated CR exceeds a pre-determined limit, the vehicle must decrease its CR below the limit. However, the specific technique to achieve this has not been standardized; it is left to the implementers to choose any of the following techniques: (a) drop packet transmission/re-transmission, (b) adapt the MCS, or (c) adapt transmission power (A. MansouriV. 2019). This work is complete throughout (a) and (c), which provides researchers the ability to precisely measure the performance of a C-V2X system that is applied to real-world scenarios.

Experimental Results

The simulation was run with the following parameters: $\lambda = 20$ (120 vehicles in total); TX power = 23 dBm; RX sensitivity = -97.28 dBm; message transmission rate = 10 Hz; and inter-broadcast interval = 100 msec. The MCS indices were set to $\{7, 11\}$ with the number of subchannels equal to 2 and 7, respectively.

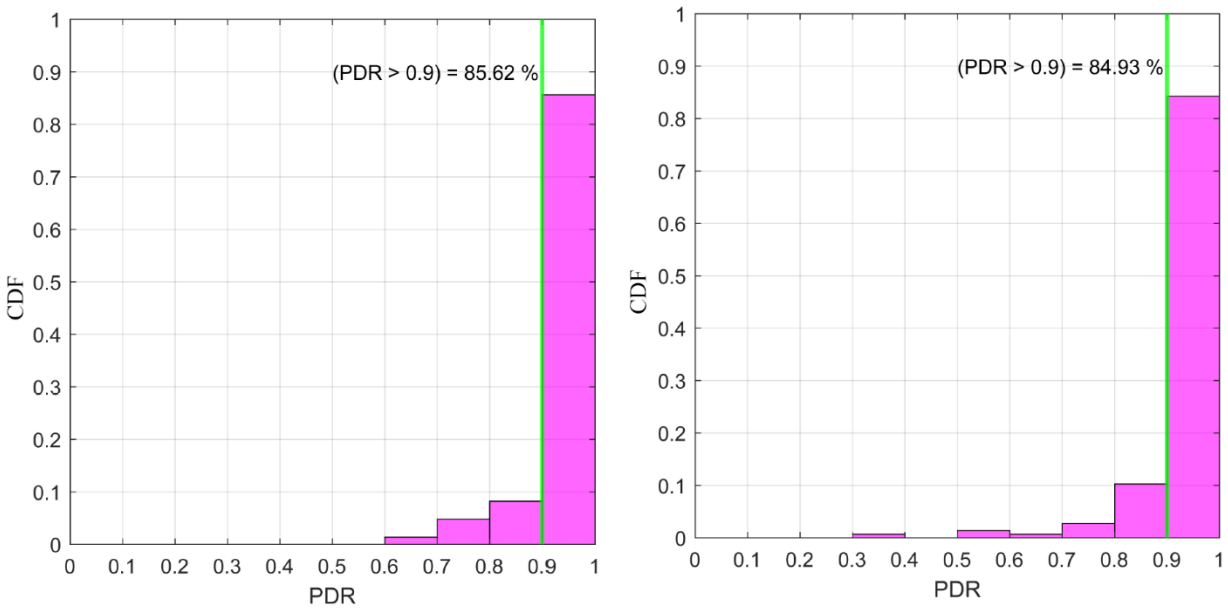

(a) MCS index = 7 (b) MCS index = 11

Figure 16. Graph. CDF of PDR

Figure 15 demonstrates the probability density function (pdf), $f_X(x)$, of the end-to-end latency x (in msec) from a RSU to a vehicle. It is evident that a higher MCS index of 11, which uses a larger number of subchannels, yields an improved latency for the vehicles compared to a lower MCS index of 7.

Although higher MCS indices are expected to offer higher data rates, the transmitted messages become more susceptible to errors due to distance from the RSU, interference, and obstacles. Recall that in the simulation, big trailer trucks and buildings are the major obstacles that result in the reduction of the overall PDR as the MCS index changes from 7 to 11.

Figure 16 demonstrates the result of PDR: it lays out a cumulative distribution (CDF) for PDR. One can find that 85.62% of the total vehicles have PDRs exceeding 0.9 in the case of MCS

index of 7, while the MCS index of 11 suppresses the percentage 84.93%, which are shown in Figures 16a and 16b, respectively. It should also be noted that with an MCS index of 11, some vehicles witness a lower PDR dropping down to 0.3, whereas with an MCS index of 7, the lowest PDR observed is around 0.6.

In-Lab Testing Development

The key digital modulation techniques are quadrature phase shift keying (QPSK) and 16-quadrature amplitude modulation (QAM). Henceforth, we built an in-lab testing suit by using two software-defined radios (SDRs) representing a TX and a RX. This single-link communication system operating at the frequency of 5.9 GHz forms the foundation of our field test capability, which shall be presented in Section <Field Test Apparatus Development>.

Via the in-lab testing by using two SDRs, we confirm that it is possible to implement a basic communications link with the help of the Gnu's Not Unix (GNU) Radio Companion software. It was successfully shown that small sequences of binary data could be transmitted and recovered using a QPSK modulation scheme despite the current inability of the link to transmit more meaningful information.

System Model

A primitive radio communication link was established by means of two SDRs, in which one radio was configured to exclusively make transmissions while the second radio exclusively

received and recovered the transmitted signals. The SDR's used to implement the link were the National Instrument (NI) Universal Software Radio Peripheral (USRP)-2954R and the Ettus USRP X310 (each equipped with a UBX-160 daughterboard), which were controlled and interfaced with by means of the software known as GNU Radio Companion installed on Raspberry Pi 4B (with a 8-GB read access memory (RAM)) microprocessors running Raspbian operating system (OS), a derivative of Debian Linux distribution. A single VERT 2450, dual-band, vertical antenna was attached to each radio to facilitate transmissions at a center frequency of 5.9 GHz, and the MATLAB computing platform was utilized as the primary means for analyzing/post-processing data stored by the RX node during testing.

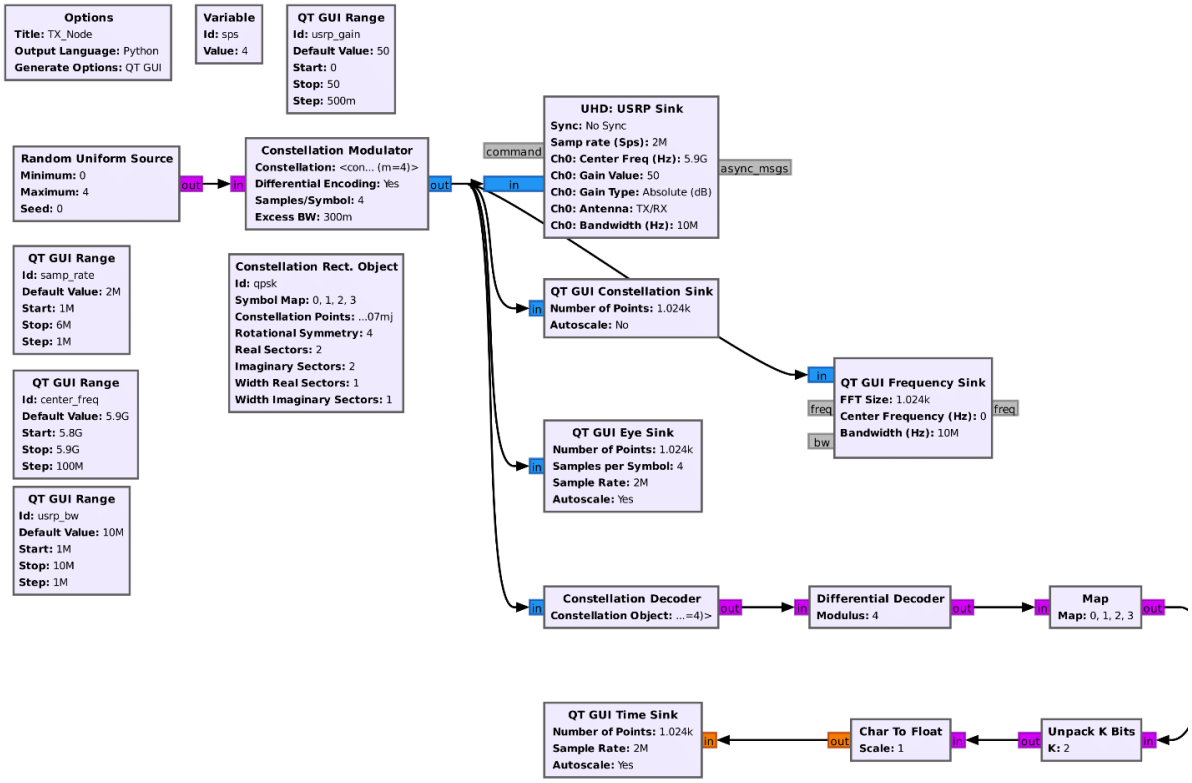

Figure 17. Flowgraph. TX node on GNU Radio Companion

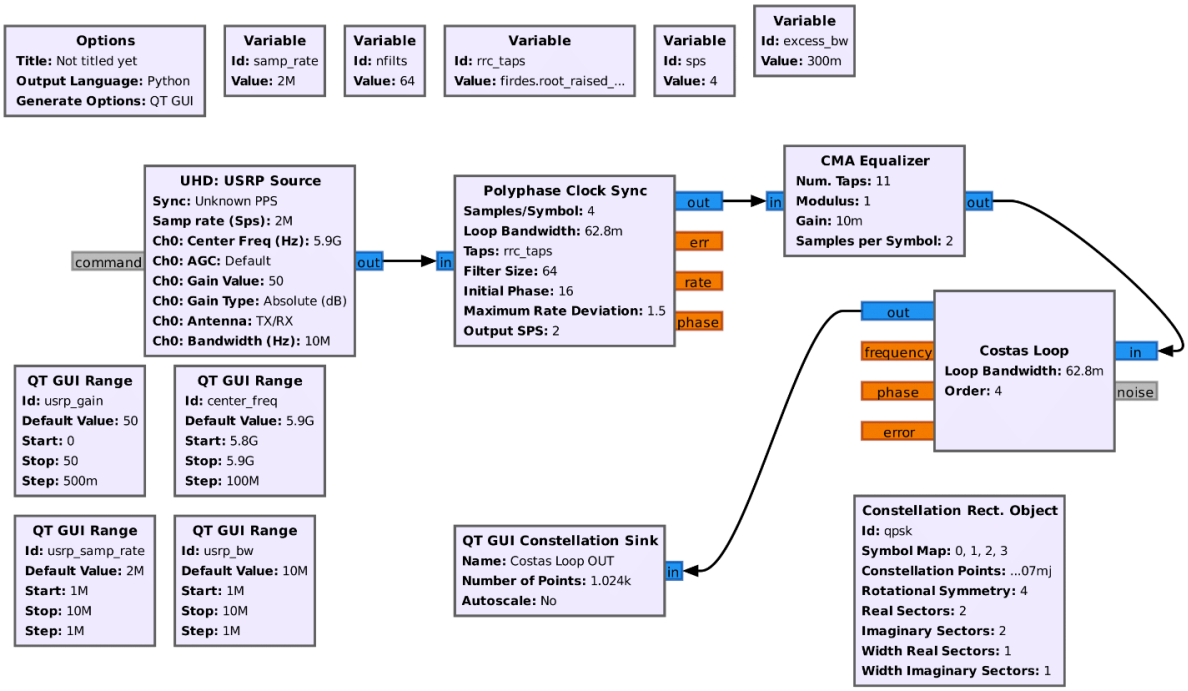

Figure 18. Flowgraph. RX node on GNU Radio Companion

GNU Radio Companion was selected for interacting with the SDR's due to its ease of use and the abundant amount of information already available for reference on the official GNU Radio Wiki and other engineering forums alike. Informational guides such as "QPSK Modulation and Demodulation" provided on the wiki page helped to form the foundation upon which the investigations described by this report were performed. The GNU Radio flowgraphs utilized during testing of the TX-RX link were derived directly from the aforementioned guide and have been adapted to accommodate the SDR hardware as required.

Testing was performed by connecting each of the SDR's to an assigned Raspberry Pi via ethernet and executing python programs produced subsequent to the implementation of the TX and RX flowgraphs in GNU Radio Companion (see Figures 4-3 and 4-4). The node responsible for transmitting performed QPSK modulation on an input before providing the modulated data to a

"USRP Sink" block, at which point the signal was transmitted by the SDR at a carrier frequency of 5.9 GHz with a bandwidth of 10 MHz. Two different data sources were utilized while investigating the link, the "Random Uniform Source" block, and the "Vector Source" block. Initial testing exclusively relied upon the Random Uniform Source of which generated random samples output in bytes with values between the parameters provided to the block. Similarly, the Vector Source was used to produce a stream of data output in bytes, however, unlike the Random Uniform Source, the data provided by the Vector Source was generated in the same order in which it was input to the block.

The flowgraph implemented to facilitate the recovery of transmitted signals began with a "USRP Source" block of which allowed for GNU Radio Companion to interact with the SDR being utilized as the receiver in the link. The USRP Source block was tuned to the same carrier frequency as that of the transmitter, 5.9 GHz, and also featured a bandwidth of 10 MHz. Signals received by the SDR were subjected to a recovery loop within the RX flowgraph prior to reaching the demodulation block/outputs (spectrum analyzer, constellation diagrams, file sink, etc.). The recovery process was absolutely critical as transmitted signals are known to experience distortion deriving from sources such as inter-symbol interference and multipath losses while traveling through a channel to the receiver. Signal recovery was facilitated by a series of blocks meant to correct distortions in the timing, phase, and frequency of the received signal such as the Polyphase Clock Sync, the constant modulus algorithm (CMA) Equalizer, and the Costas Loop.

All testing was performed with the SDR's positioned approximately two feet apart from antenna to antenna as to mitigate losses to the maximum extent possible without needing to exceed the

gain limits of the radios defined by the aforementioned USRP Source and Sink blocks. The environment in which the tests were performed included standard appliances (televisions, monitors, Wi-Fi routers, etc..) within a close proximity, however, no nearby devices were known to be operating at the 5.9 GHz range during experimentation. Testing was always initiated by executing the transmitting program implemented at the TX node. Once transmissions had begun, the program that facilitated the recovery of the transmitted signals was executed. For tests that involved storing data, the recovery program was terminated after approximately 10 seconds worth of run time due to the high volume of data that was typically stored during each trial. The results of the tests were captured/stored for post-processing and analysis.

Experimental Results

The experimental results produced subsequent to testing the radio link are given by spectrum analyzer outputs, eye diagrams, constellation diagrams, and raw binary data of which have been categorized with respect to the data source utilized during the trial from which the given result derives from. As such, the results of the investigation thus far were produced when either the Random Uniform Source or the Vector Source blocks provided input to the TX node. Given below are the plots produced by the receiver and the binary data (Vector Source case only) that was stored and evaluated using the MATLAB software environment.

Figures 4.5 through 4.7 display the spectrum, constellation diagram, and eye diagram produced by the receiver during recovery of a transmitted signal when the input to the TX node was generated by the Random Uniform Source block with a range of values: [0,4). Each of the diagrams represent

the transmitted signal as expected with the constellation diagram (Figure 4.6) clearly displaying four distinctly mapped symbols of which is a prominent characteristic of a QPSK modulation scheme.

Similarly, Figures 4-8 through 150 display the results produced when the Vector Source block was used to provide input sequence, 0, 1, 2, 3 (Sequence 1), to the TX node. As expected, the spectrum and constellation/eye-diagrams resembled that of those produced during the trials involving the Random Uniform Source block, each of which are indicative of a successful transmission/recovery.

To further verify that the data being transmitted by the link was being recovered successfully, a sample of the recovered data was stored during one of the trials of the experiment involving Vector Source Sequence 1 (0, 1, 2, 3). Subsequent to accessing the binary file produced by the receiver using MATLAB, it was confirmed that the sequence had been transmitted and recovered as anticipated. We stored the binary data at the receiver during such trials, so it displays one full iteration of Sequence 1. The data reveals that the sequence was not correctly recovered when the receiver was first activated. This is a significant observation as it provides important insight into how a QPSK communication system sometimes operates. In the case of the recovery loop implemented at the RX node (see Figure 18), a short period of time was required to pass while the loop synchronized with the transmitted signal before the recovered data could be recognized as the original sequence.

In attempt to expand upon the capabilities of the still very primitive communication system, another sequence (denoted as Sequence 2) was passed to the Vector Source block as follows: 0,

255, 72, 101, 108, 108, 111, 87, 111, 114, 108, 100. The first two values in the sequence, 0 and 255, were included as an attempt to mark the beginning of each iteration of which could be identified during post-processing analysis in MATLAB. The rest of the sequence can be translated using a standard American Standard Code for Information Interchange (ASCII) table to reveal the message, “Hello World.” The results of the tests involving Sequence 2 are given by Figures 15-1 through 15-3 in which it is clear that the signal was not recovered correctly. The constellation and eye diagrams reveal a considerable amount of distortion, and the binary data (not pictured) did not exhibit any recognizable patterns in line with the predetermined sequence.

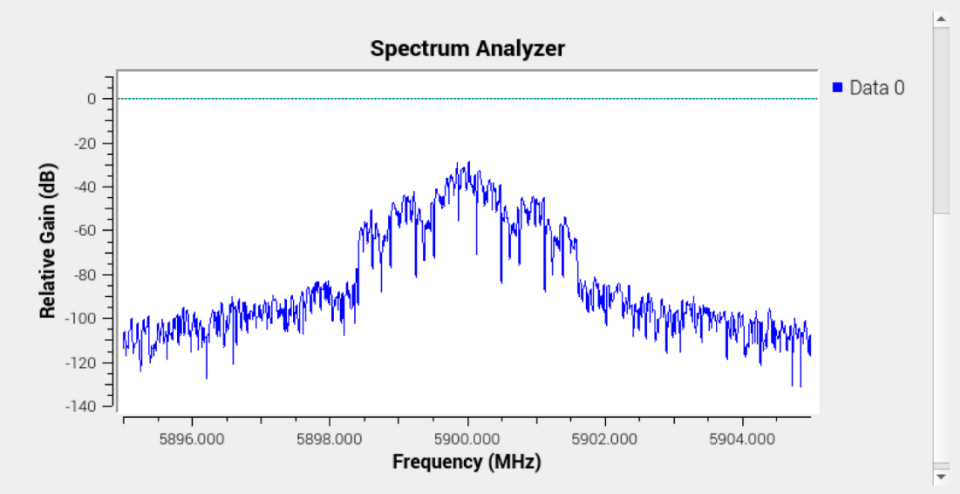

Figure 19. Plot. Random Uniform Source–Spectrum analyzer output

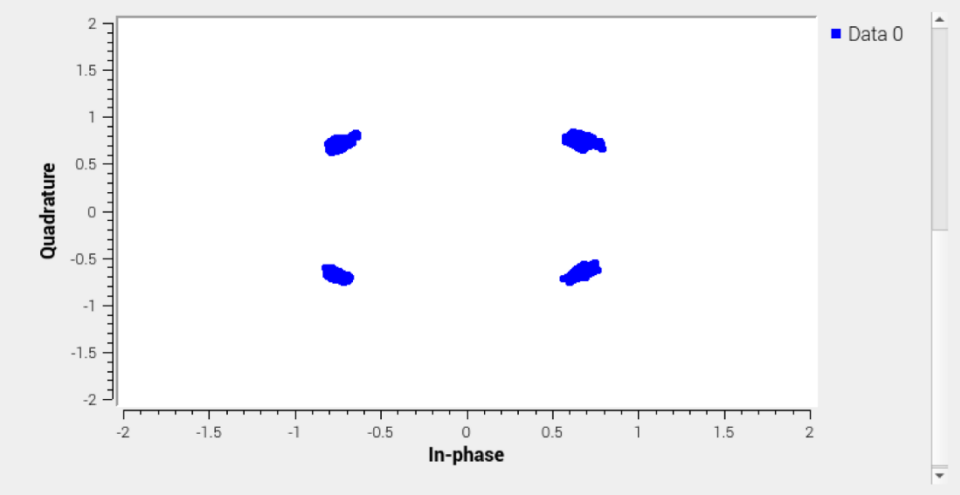

Figure 20. Plot. Random Uniform Source–Constellation diagram

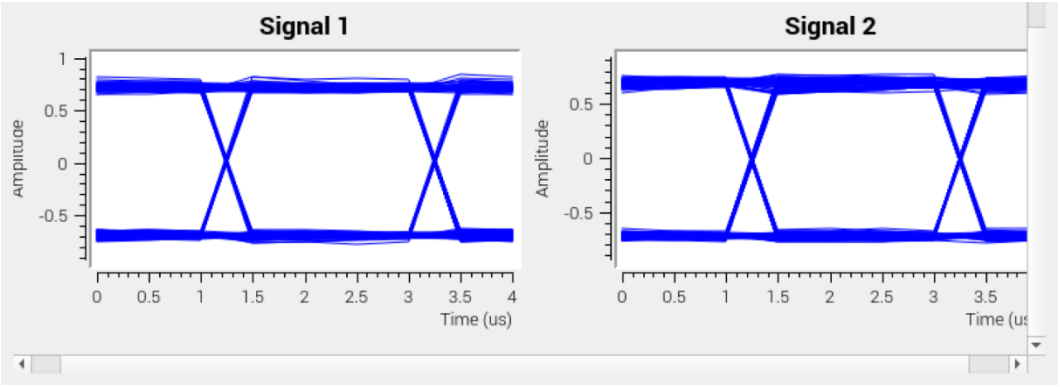

Figure 21. Plot. Random Uniform Source–Eye diagram

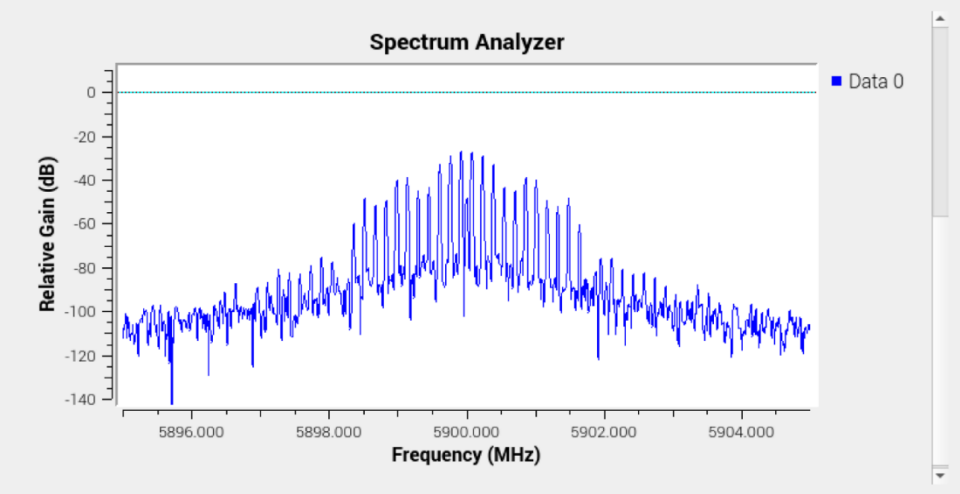

Figure 22. Plot.Vector Source–Sequence 1: Spectrum analyzer output

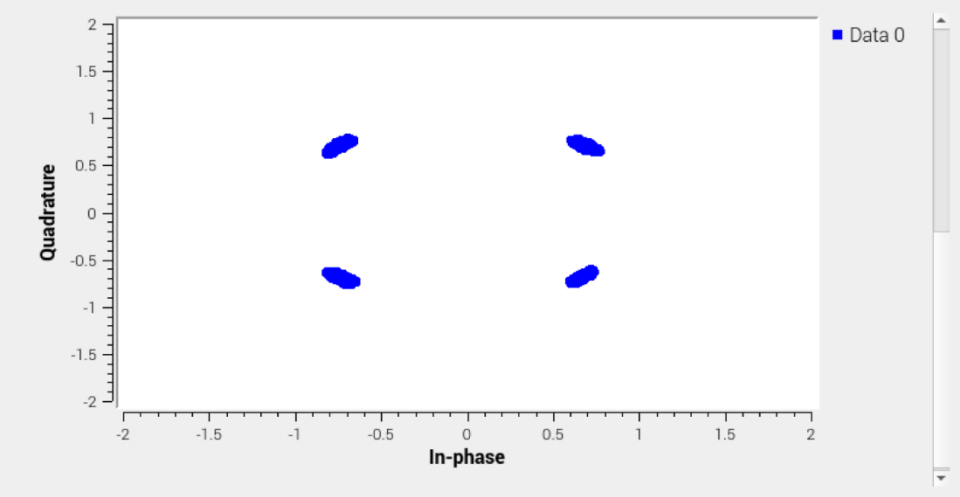

Figure 23. Plot. Vector Source–Sequence 1: Constellation diagram

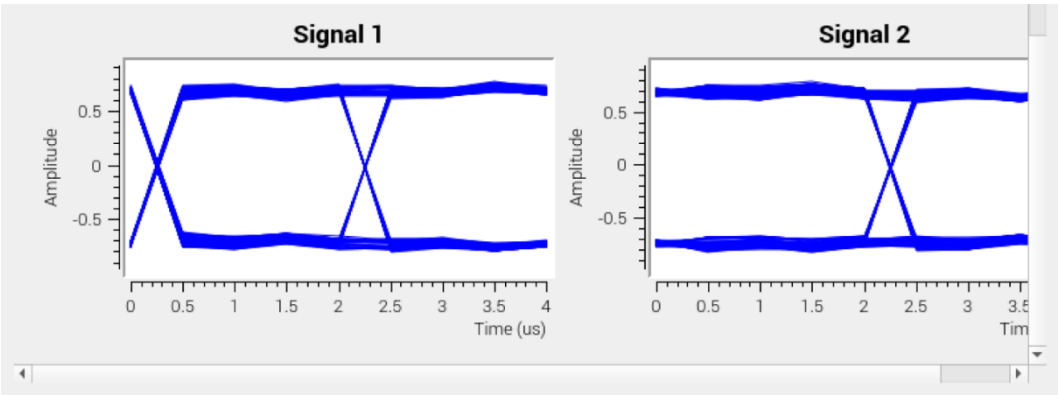

Figure 24. Plot. Vector Source–Sequence 1: Eye diagram

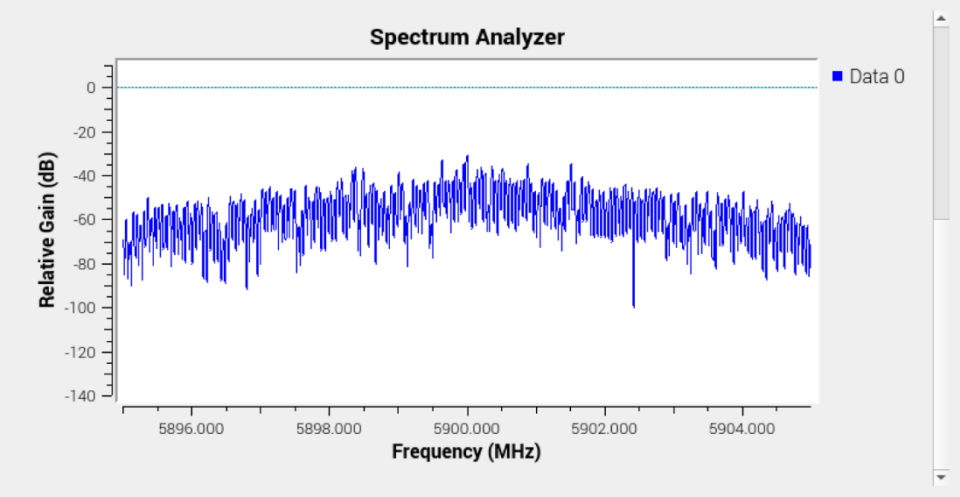

Figure 25. Plot. Vector Source–Sequence 2: Spectrum analyzer output

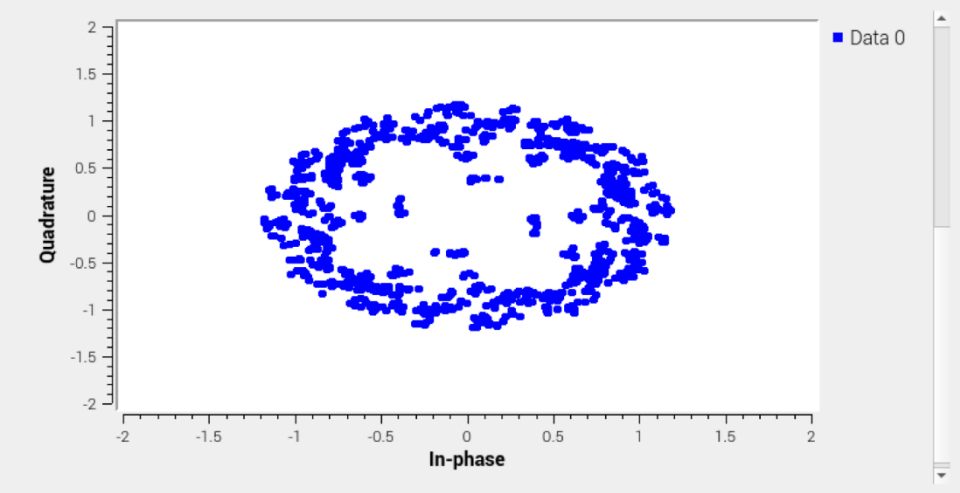

Figure 26. Plot. Vector Source–Sequence 2: Constellation diagram

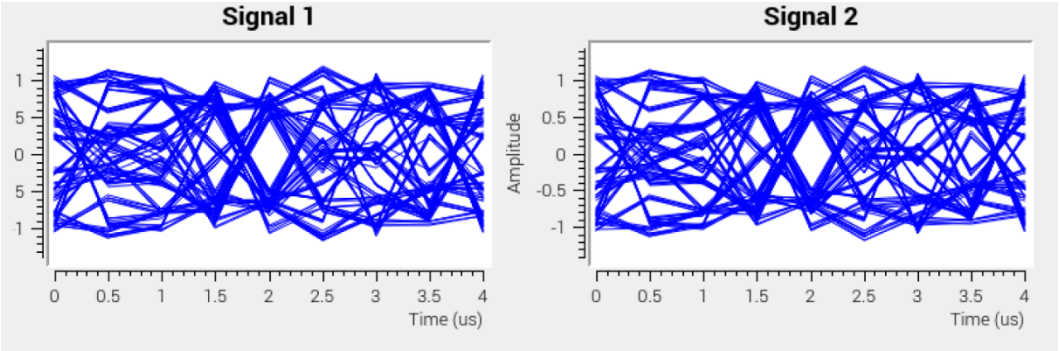

Figure 27. Plot. Vector Source–Sequence 2: Eye diagram

Field Test Apparatus Development

Notice that the contents laid out in this section are collected from a field test on a RSU currently operating in DSRC. However, we emphasize that the digital modulations schemes--viz., QPSK and 16-QAM--are in common between DSRC and C-V2X; thus, the result presented in this section holds the generality to be applied to C-V2X.

An initial “field test” was performed, during which a USRP SDR was positioned approximately 20-30 yards from an active RSU as an attempt to “sniff” radio emissions coming from the unit. Using two different GNU Radio based programs for monitoring a frequency spectrum centered at 5.9 GHz, transmissions made by the road-side unit were detected with a limited degree of success. The spectrum analyzer software revealed that the unit did in fact appear to be actively making transmissions of which occurred in short bursts on what seemed to be no specific intervals. Images of the test set-up/environment are given below as to further illustrate the scenario in addition to images featuring captures of the spectrum analyzer taken during testing.

The RX flowgraph that has been developed via this task, which demodulates and recovers QPSK modulated signals was also executed during the field test. However, because the RSU made very brief/discontinuous transmissions, the recovery loop implemented within the flowgraph was never able to synchronize with the signals displayed by spectrum analyzer. Therefore, the constellation diagram that was produced appeared as if there were no transmissions being made at the specified frequency as depicted in Figure 11 below.

Figure 28. Photo. Field test setup (A SDR (the white box), a Raspberry Pi as a device hosting the SDR (the black box on the SDR), and a portable display (the orange box))

Figure 29. Photo. The field test setup from a different angle

Figure 30. PhotoGDOT RSU located at South Main St and Tillman Rd in Statesboro, GA

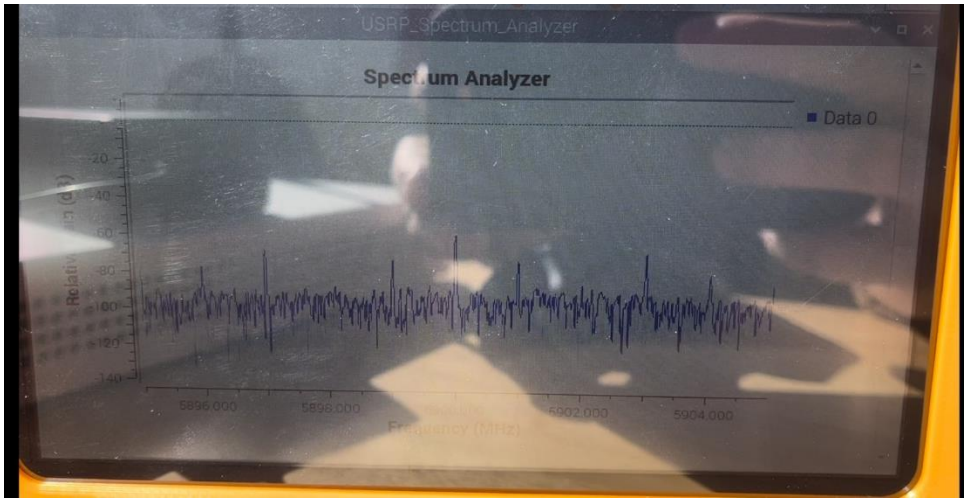

Figure 31. Photo. Spectrum Analyzer – Spikes at 5.897 and 5.903 GHz

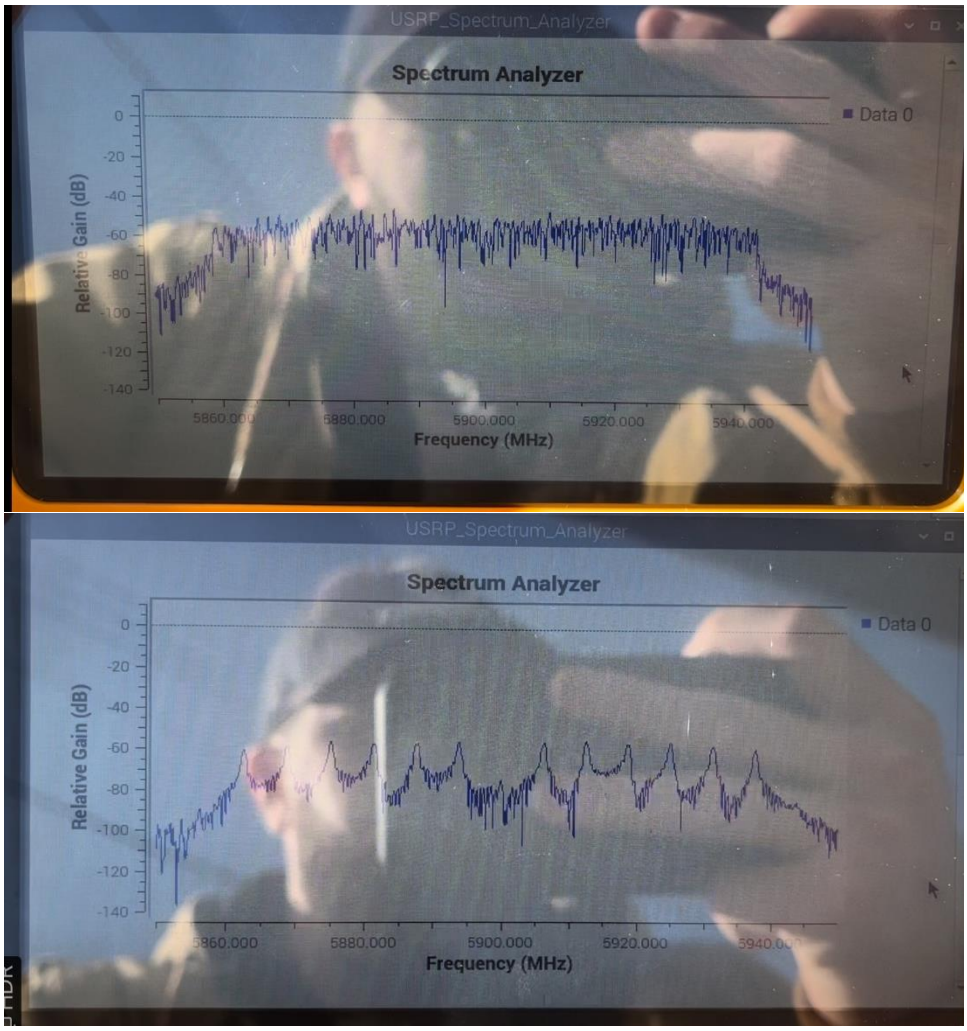

Figure 32. Photo. Spectrum Analyzer -- Snapshots of a pulse with bandwidth of 100 MHz and power of 40+ dB

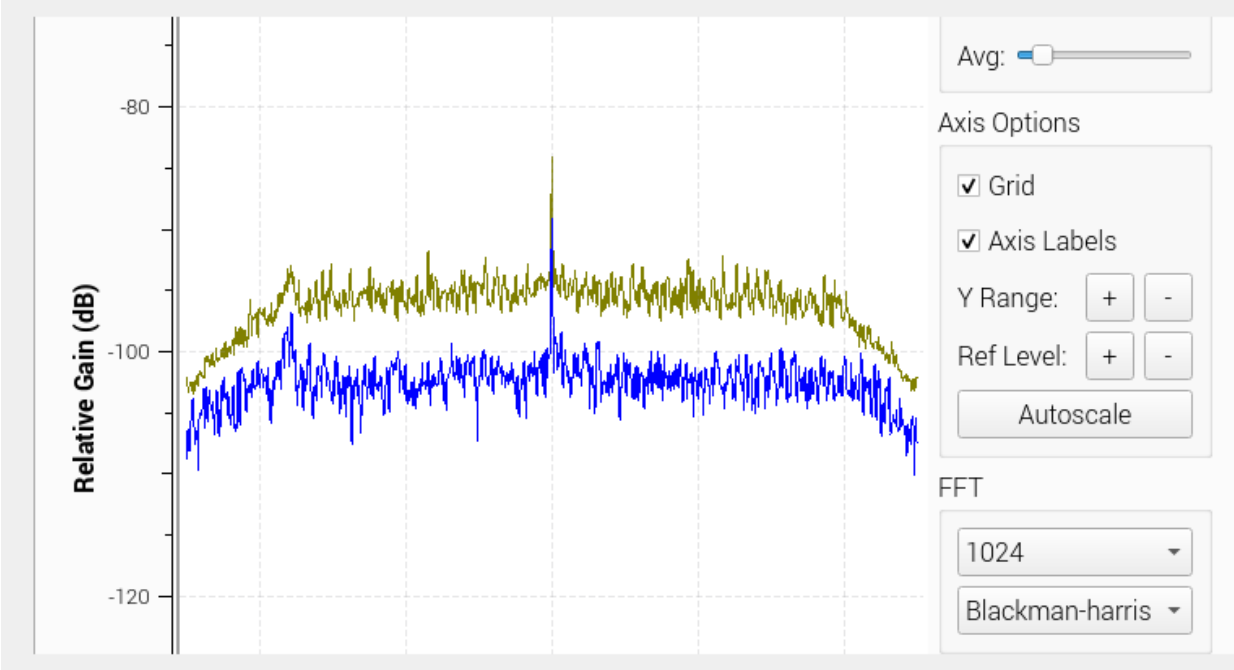

Figure 33. Plot. FFT plot on GNU Radio

Chapter 5. Task 4: 30 MHz Application Map

This task is dedicated to investigating the impacts of the U.S. FCC's decision to constrain the 5.9 GHz band for ITS to 30 MHz from 75 MHz. The Commission decided to reallocate the spectrum band that used to be dedicated to V2X uses and to leave only 40% of the original chunk (i.e., 30 MHz of bandwidth) for V2X. It ignited concern of whether the 30-MHz spectrum suffices key V2X safety messages and the respective applications. Via this task, we lay out a comprehensive investigation into various safety message types and their corresponding latency requirements. Our study encompasses an extensive study of PDR and latency across varying vehicular densities and quantities of RSUs. Furthermore, we provide simulation outcomes that scrutinize the feasibility of accommodating these rates within the 30-MHz spectrum configuration.

Background

Motivation

V2X technology allows vehicles to communicate with other vehicles, infrastructure, and vulnerable road users to enhance safety, thereby preventing traffic crashes, mitigating fatalities, alleviating congestion, and reducing the environmental impact of the transportation system (US Department of Transportation 2017). This capability gives V2X communications the central role in the constitution of ITS for connected vehicle environments. The full 75 MHz of the 5.9 GHz spectrum band (5.850-5.925 GHz) has long been reserved for intelligent transportation services such as V2X technologies. Nonetheless, the U.S. FCC voted to allocate the lower 45 MHz (i.e., 5.850-5.895 GHz) for unlicensed operations to support high-throughput broadband applications

(e.g., Wireless Fidelity, or Wi-Fi) (US FCC Dec. 2019.). Moreover, the reform went further to dedicating the upper 30 MHz (i.e., 5.895-5.925 GHz) for C-V2X as the only technology facilitating ITS. To this line, we deem it prudent to evaluate *what is possible in a limited 30 MHz spectrum* to ensure that the ITS stakeholders can continue to develop and deploy these traffic safety applications.

Limitation of Prior Art

C-V2X has been forming a massive body of literature. Nonetheless, only little attention was paid to the feasibility of C-V2X in the reduced 30 MHz spectrum for safety applications. The end-to-end per-packet latency, defined as the time spent by a successful packet to travel from its source to final destination, is a classical networking metric. An advanced latency metric--namely, the inter-reception time (IRT)--was proposed, which measures the time length between successful packet deliveries (ElBatt, et al. 2006). However, we find the IRT to have limited applicability as it becomes efficient in broadcast-based safety applications only. Considering the variety of our target applications, this research employs PDR and the classical latency as the main metrics, as shall be detailed in Section <Simulation Results>.

Now, in regard to the characterization of a V2X system, the literature introduced a wide variety of proposals. Several approaches were compounded into large bodies such as theoretical/mathematical approaches (L. CaoS. 2023), simulation-based (WeiR. 2022), and channel sounding-based (M. AkdenizY. 2014). The prior art certainly provides profound insights; yet it is not directly conclusive whether the reduced 30-MHz bandwidth makes it feasible to operate C-V2X on realistic road and traffic scenarios. The same limitation can be

found in the current literature of V2X safety-critical applications (C. ZoghlamiR. 2022): the proposals lay out approaches to support such applications but leave it unaddressed what the influence will be after the C-V2X got deprived of 60% of its bandwidth.

Contribution of This Research

This research aims to assist the ITS literature in regard to operating C-V2X technologies in such an environment. As such, rather than final nor conclusive, this work should be regarded an initiative, igniting further tests and assessments on the impact of 30 MHz environment on the application deployment. Provided that, we extend the C-V2X literature on the following fronts:

- Pioneer to clarify the feasibility of safety-critical applications in the reduced 30 MHz spectrum setting
- Develop a quantification framework for C-V2X performance in a comprehensive but easy manner to maneuver
- Identify message types associated with safety-critical applications

System Model

Spatial Setup

Figure 10 illustrates an urban environment setup that was used in this research's simulations (SAE, Vehicle level validation test procedures for V2V safety communications 2022). A two-dimensional space $\mathbb{R}^2$ is supposed, which is defined by the dimensions of 520 m and 240 m for

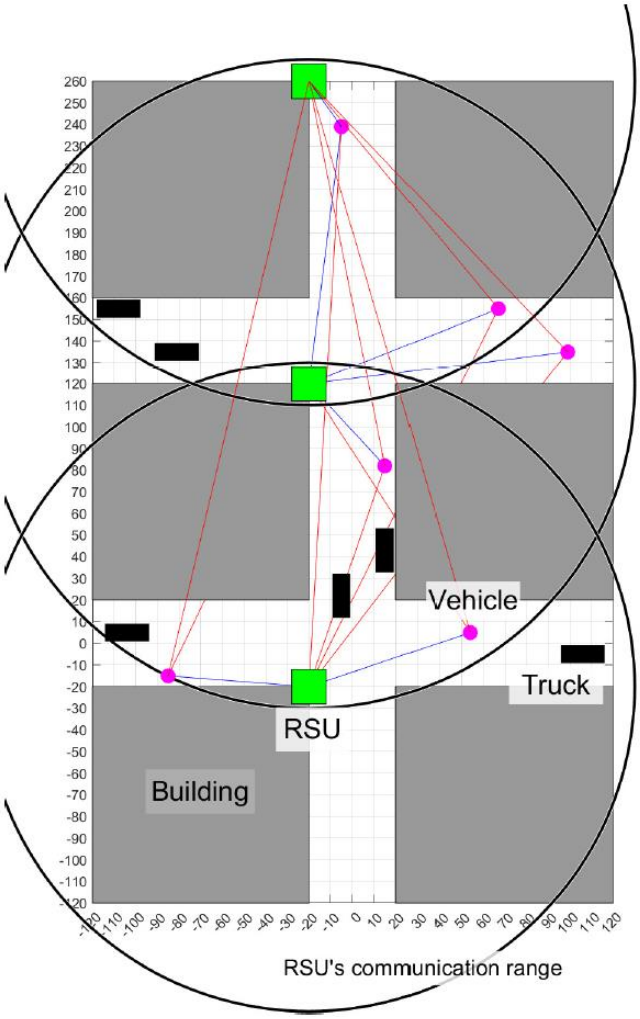

Figure 34. Simulation. Geometrical setup of the proposed simulator (with vehicle density of $\lambda = 1$ in the entire system space)

the north-south and the east-west axes, respectively. The RSUs are marked as green squares and the range of operation of each RSU is set to 150 m, indicated by a black circle around each RSU.

There are two types of physical obstacles: trailer trucks (marked as black rectangles) and buildings (drawn as big gray squares). Moreover, we suppose *two junctions* (rather than just one) as an effort to examine any possible interference between roadside units (RSUs) on the C-V2X performance as each junction is equipped with a RSU. The connection from a RSU to a vehicle is shown by either a red or blue line: the red indicates a "blocked" connection whereas the blue means a "connected" link. The blockage can be caused by physical obstacles, viz., a building or a large trailer truck that are displayed by a large gray square and a black rectangle, respectively.

The distribution of the vehicles follows a *homogeneous PPP* in $\mathbb{R}^2$. We define a general situation where a safety-critical application disseminates a message of its respective type over a C-V2X

network. (See Section <Setup and Parameters> of Chapter 3 for details on the message types.) Unlike vehicles, RSUs are located at each junction (ForsterT. 2022). Furthermore, the symbols λ and θ are employed to indicate the densities of vehicles and trucks per road segment, correspondingly. A total of three road segments exist, each of which is comprised of two directions, wherein each direction consists of two lanes. As such, six directions are considered in total: viz., South-North, North-South, East-West 1, East-West 2, West-East 1, and West-East 2. According to the densities λ and θ, the probability of signal being blocked varies, which, in turn, influences the end-to-end latency of a message. For instance, a large λ and a large θ yield a higher level of competition for medium and an increased level of physical signal blockage, which therefore elevates the latency accordingly. It is also noteworthy that each vehicle, upon reaching the end of a road, starts over from the opposite end of the same lane. This setup is to keep the total number of vehicles constant at all times, as a means to maintain the same level of competition for the medium at any given time and thus guarantee the accuracy for further stochastic analyses.

Communications Parameters

This research adopts the 3GPP Release 15 Long Term Evolution (LTE)-V2X for the PHY (3GPP, 5G; Study on channel model for frequencies from 0.5 to 100 GHz 2022) and radio resource control (RRC) functions (3GPP, LTE; Evolved Universal Terrestrial Radio Access (E-UTRA); User equipment (UE) radio transmission and reception 2023). We assume *Mode 4* communication takes place directly between vehicles and the RSUs without going through a cellular network. Direct communication is enabled through sidelink which is crucial for providing services like basic safety messages and traffic advisories. Mode 4 is specifically designed for low-latency and high-reliability communication, making it suitable for safety-

critical applications like collision avoidance. Nonetheless, we claim that the versatility of our simulation framework can easily be extended to accommodate NR-V2X as well. To elaborate on the sidelink of LTE-V2X, our simulation implements the key channels (3GPP, LTE; Evolved Universal Terrestrial Radio Access (E-UTRA); User equipment (UE) radio transmission and reception 2023), namely the Physical Sidelink Control Channel (PSCCH) for transmitting physical layer sidelink control information (SCI); the Physical Sidelink Shared Channel (PSSCH) which is responsible for carrying Transport Blocks (TBs) of data; and the Physical Sidelink Broadcast Channel (PSBCH) for broadcasting BSM.

We suppose that all the vehicles distributed in $\mathbb{R}^2$. have the same ranges of carrier sensing and communication. The possible subchannel sizes as defined by 3GPP LTE specification 36.213 (3GPP, LTE; Evolved Universal Terrestrial Radio Access (E-UTRA); Physical layer procedures 2022) are $\{4, 5, 6, 8, 9, 10, 12, 15, 16, 18, 20, 25, 30, 48, 50\}$ RBs, and the number of subchannels can be $\{1, 3, 5, 10, 15, 20\}$. As such, this research supposes 50 RBs per subchannel, which matches our assumption of 10 MHz per channel. Furthermore, since a city road environment is considered for the simulation as shown in Figure 34, the Urban Micro (UMi)-Street Canyon path loss model (3GPP, 5G; Study on channel model for frequencies from 0.5 to 100 GHz 2022) is implemented. However, we reiterate that our simulation can easily accommodate other path loss models defined in the standard.

Proposed C-V2X Performance Evaluation Framework

Message Types

Table 3 categorizes several representative message types (i.e., as the last row) according to the "traffic families" (i.e., as the 3rd row). We particularly highlight that the ongoing SAE J3161 standardization activity (SAE, Vehicle level validation test procedures for V2V safety communications 2022) is primarily based on the end-to-end latency, namely, the packet delay budget (PDB). Discussion on the metric selection shall be revisited in Section <Metrics>. We assign different ProSe per-packet priorities (PPPP) (3GPP, Universal Mobile Telecommunications System (UMTS); LTE; Proximity-based services (ProSe); Stage 2 2022) based on the importance of a message type. This proposition is to further extension to optimization of C-V2X via assigning different communication profiles (viz., number of subchannels, MCS, number of retransmissions, etc.) for the packets based on packet size, velocity, and CBR.

Table 3. Mapping of message types to traffic priority levels

Service Type	Safety Services				Mobility Services		
Traffic Direction	V2V		V2I-I2V		V2I-I2V		
Traffic Families	Critical V2V	Essential V2V	Critical V2I-I2V	Essential V2I-I2V	Transactional	Low-priority	Background
Minimum PPPP	2	5	3	5	6	6	8
Minimum PDB	20 msec	100 msec	100 msec	100 msec	100 msec	100 msec	100 msec
Example Messages	BSM, EVA	BSM	RSM, MAP	SPaT, RTCM	SSM, SRM	TIM, RWM	TCP, UDP

Table 3 shown above can be elaborated as follows (SAE, V2X communications message set dictionary 2020, USDOT, CV273: Introduction to SPaT / MAP messages 2023): BSM, emergency vehicle alert (EVA), road safety (RSM), map data (MAP), signal phase and timing (SPaT), Radio Technology Commission for Maritime Services corrections (RTCM), signal status (SSM), signal request (SRM), traveler information (TIM), and road weather (RWM), as well as even transport-layer protocols such as transmission control (TCP) and user datagram (UDP). These types of messages support a broad set of V2V and vehicle-to-infrastructure (V2I)

applications, e.g., forward collision warning, pre-crash sensing, emergency vehicle warning and signal preemption, and infrastructure-to-vehicle warning messages.

As found from the "V2V" column of Table 3, some applications operate based on the same message types, allowing numerous applications to be operated without requiring additional spectrum. However, different applications using the same message types can have vastly different spectrum needs due to differing message sizes and frequency of message transmission, so there are scenarios in which some applications using the same message types could and could not be deployed. Additionally, the available spectrum will be dependent in part on the number of vehicles within communication range and the types of applications operating in a given area. Because of this, it will likely be necessary to establish a scheme that prioritizes safety-critical applications while underrating non-safety-critical applications in such situations.

Simulator Development

This proposed research features *integration* of the LTE-V2X PHY and RRC simulator with two other major simulators: namely, the geographic environment simulator (D. SunuwarS. 2023) and a virtual reality (VR)-based driving simulator (Z. ReyesS. 2023). Figure 35 illustrates how this integration is achieved.

LTE-V2X Simulator

The simulator developed via this research features integration of key functions defined in 3GPP standards for the LTE-V2X PHY and RRC layers. As such, it effectuates the sidelink

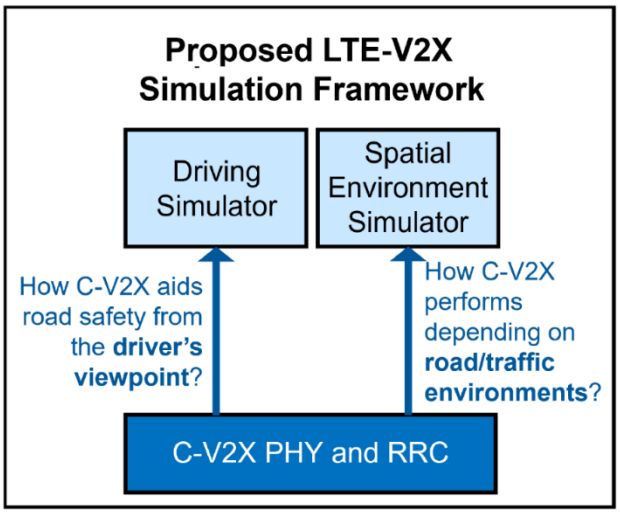

Figure 35. Framework. Structure of the proposed simulator

communications among the vehicles and RSUs, following major TRs and TSs of the 3GPP Release 15 standard (3GPP, LTE; 5G Overall description of Radio Access Network (RAN) aspects for Vehicle-to-everything (V2X) based on LTE and NR 2022).

Semi-persistent scheduling (SPS) is employed to allocate subchannels from the resource pools of PSSCH and PSCCH. Various time interval options between packets are provided: 20, 50, 100, 200, 300 ... 1000 msec, which correspond to transmission rates of: 50, 20, 10, 5, ... 1 Hz (A. MansouriV. 2019). Once a vehicle opts for a new resource, it reserves this resource for a specified number of iterations, as indicated by the resource re-selection counter (RC). Different sets of RCs are available based on the chosen interval: for intervals of 100, 50, and 20 msec, the respective RCs are [5,15], [10,30], and [25,75] (A. NabilK. 2018). For our simulation, we have chosen a 50 msec time interval between packets, yielding a transmission rate of 20 Hz and an RC range of [10,30]. The RC is chosen randomly within the range of 10 to 30 and decreases by one following each transmission. When the RC reaches zero, the resources become available for new vehicles to utilize. This LTE-V2X simulator forms the basis for two other major components of the proposed simulation framework—viz., spatial environment simulator and driving simulator.

Spatial Environment Simulator

On top of the *LTE-V2X simulator*, the spatial environment simulator facilitates an urban environment shown in Section <Spatial Environment Simulator>. As Figure 35 depicts, the existence of this spatial environment component adds the context of *the C-V2X performance in different road/traffic settings*. We emphasize that this component will be strengthened by adding a wider variety of road environments and traffic scenarios. The *LTE-V2X simulator* and the *spatial environment simulator* are both developed using MATLAB. Numerous parameterized variables are established, allowing for the adjustment of factors such as RSU quantity, vehicle density, truck density, vehicle speed, subchannel RBs count, inter-packet transmission intervals, and more.

Driving Simulator

The driving simulator that puts a human user into a 1st-person driving setup. That way, the user can have *live experience of connected vehicles*: the experience can actualize the user on how car-to-car connections can promote the safety in various traffic scenarios and road conditions. The simulation platform comprises three primary software modules: (i) RoadRunner, responsible for generating maps and managing traffic signals; (ii) SUMO, which handles routing for both vehicles and pedestrians; and (iii) CARLA, facilitating simulations and real-time analysis using a customized variant of Unreal Engine 4 (UE4). As shall be elaborated in Section <Numerical Results>, this driving simulator will also play the role of adding realistic contexts to V2X simulations, which clearly highlights the unique contribution of this research. We combine all of those so the user can not only (i) deploy vehicles, RSUs, and obstacles but (ii) promptly quantify the C-V2X performance out of the scenario.

LTE-V2X Congestion Control Mechanism

For guaranteeing efficient throughput and equitable allocation of resources to connected vehicles, the utilization of a congestion control mechanism becomes paramount. As emphasized in (ETSI 2018), each vehicle's ability to utilize multiple RBs per subchannel is contingent on network congestion--more in sparsely populated scenarios and fewer in densely populated contexts. Meticulously addressing specifics, the metrics of CBR and CR are defined by LTE-V2X, serving as foundations for the deployment of the congestion control mechanism. Various decentralized congestion control (DCC) approaches are discussed in (A. MansouriV. 2019, O'DriscollB. 2022). However, given our overarching goal of assessing the impact of latency across varying vehicle density and RSU count, we employ a simplified version of the congestion control mechanism outlined in Section 4.2 of ETSI TS 103574 (ETSI 2018). In our simulation, as vehicle density increases--indicating a higher number of vehicles--the RBs per subchannel are halved, ensuring a more equitable resource distribution among vehicles within range. Consequently, this adjustment could potentially compromise the resilience and dependability of the transmitted messages.

Metrics

What does it take to call the V2X performance "enough"? It is critical to address this question in order to address what this research asks: *is 30 MHz enough for C-V2X Mode 4?* We stress that this research adopts the *end-to-end latency* as the primary and the PDR as the secondary performance metric measuring a C-V2X system.

End-to-End Latency

The end-to-end latency is the length of maximum allowed time between the generation of a message at the transmitter's application and the reception of the message at the receiver's application (M. GarciaA. 2021). As this research focuses on Mode 4 of the C-V2X, we implement the latency as the length of time taken from the generation of a message at an application (of those listed in Table 3 at a RSU to the reception of the message by a vehicle. Here is the justification of "why" the latency is chosen as the key performance metric in this research over other metrics. First and foremost, the 3GPP 5G Service Requirement also identifies the end-to-end latency as one of the most critical performance indicators (3GPP, 5G; Service requirements for enhanced V2X scenarios 2022), based on which other requirement factors are defined. Not only that, the ongoing SAE J3161 standardization activity (SAE, Vehicle level validation test procedures for V2V safety communications 2022) is almost solely based on the latency, i.e., PDB.

Near-Crash Rate

We also reiterate that this research features the integration with driving simulator. We measure the *near crash rate* after a sufficiently large number of driving simulations on human subjects. Notice that a near-crash is defined as any circumstance that requires a rapid, evasive maneuver by the subject vehicle, or any other vehicle, pedestrian, cyclist, or animal to avoid a crash (NHTSA, The 100-car naturalistic driving study: Phase II -- Results of the 100-car field experiment 2006). A rapid, evasive maneuver is defined as a steering, braking, accelerating, or any combination of control inputs that approaches the limits of the vehicle capabilities. This

helps add contexts on how the improved performance of C-V2X can *actually affect the road safety*. More details on the simulation scenario follows in Section <Numerical Results>.

Packet Delivery Rate (PDR)

The calculation of the PDR involves examining the proportion of packets that have been effectively decoded in comparison to the complete count of packets sent to all the vehicles by an RSU. A packet is classified as having been successfully received if there exists no overlap between the subchannel(s) utilized for its transmission and the subchannel(s) concurrently occupied by other transmitted packets within the same subframe. It's important to note that this assessment is conducted for each unique TX-RX pair, signifying the specific interaction between the sender and receiver. For instance, if an RSU disseminates an identical message to ten vehicles, this action contributes to the packet count by ten instances. Several factors influence the PDR, including variables such as the quantity of subchannels, the interval for resource reservation, and the likelihood of resource reselection, as outlined in (A. NabilK. 2018). However, in our simulation, we have incorporated the impacts of the first two factors.

Numerical Results

Parameters

Table 4 summarizes the key parameters that were used in our C-V2X simulation. Notice from the table that we assume 50 RBs per subchannel, which occupies 180 kHz/RB × 50 RBs/subchannel ≈ 9 MHz and thus takes up most of an entire 10-MHz channel considering 1.25 MHz of a guard band (3GPP, 5G; Service requirements for enhanced V2X scenarios 2022). The vehicle density

is another noteworthy parameter: $\lambda = \{10,20,30\}$ vehicles per direction equal $\{60,120,180\}$ vehicles in $\mathbb{R}^2$, which in turn indicate $\{24,12,6\}$ m of minimum and $\{38,19,9\}$ m of maximum inter-vehicle distance. As such, we intend that $\lambda = \{10,20,30\}$ vehicles per direction represent the $\{low, medium, high\}$ vehicle density, respectively.

Table 4. Key parameters for simulation

Parameter	**Value**
Inter-broadcast interval	50 msec
Bandwidth per channel	10 MHz
Number of RBs per subchannel	50
Number of subchannels per message	1
Payload length	40 bytes
Vehicle density	{10,20,30} vehicles/direction
Number of RSUs	{1,2,3}
TX power	23 dBm
RX sensitivity	-180.5 dBm
Message TX rate	20 Hz

C-V2X Latency and PDR Results

Each subfigure in Figure 36 presents $f_X(x)$, the probability density function (pdf) of the RSU-to-vehicle latency x in miliseconds (msec). The pdf is compared to the latency requirements of 20 msec as red vertical line that has earlier been discussed in Table 3. Via the comparison, Figure 36 displays very clearly *how many vehicles generated in the* $\mathbb{R}^2$ *are able to support which message types and applications*. Vertical comparison in a single column indicates that a higher vehicle density yields a higher latency and thus a higher chance of exceeding the 20 msec latency requirement. Horizontal comparison in a single row implies that a larger number of RSUs (each taking a full 10-MHz channel) gives a lower latency and thus a lower probability of exceeding

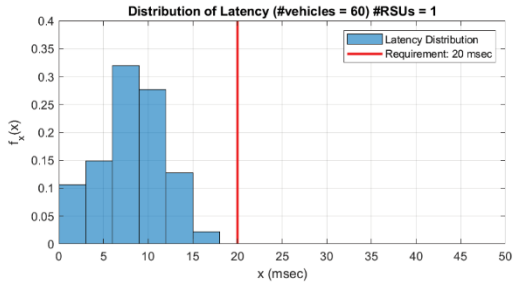

(a) 1 RSU and 10 vehicles/direction

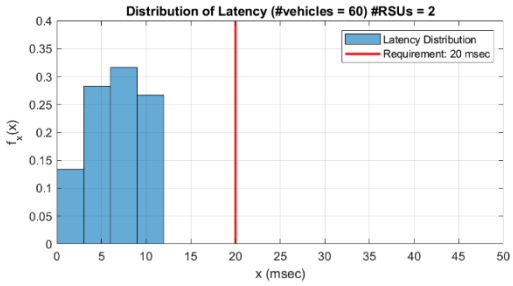

(b) 2 RSUs and 10 vehicles/direction

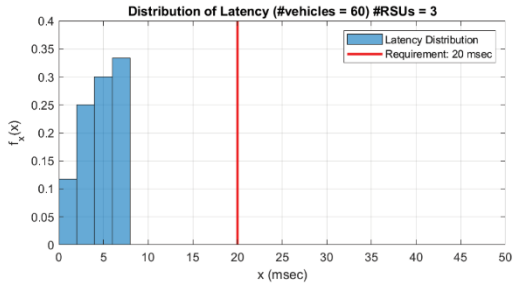

(c) 3 RSUs and 10 vehicles/direction

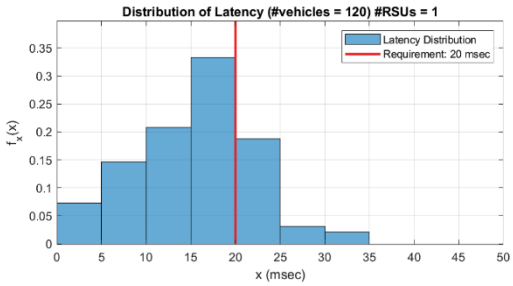

(d) 1 RSU and 20 vehicles/direction

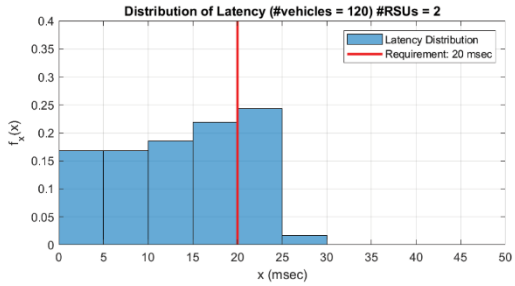

(e) 2 RSUs and 20 vehicles/direction

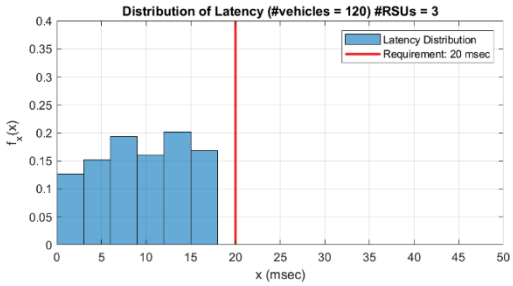

(f) 3 RSUs and 20 vehicles/direction

Figure 36. Plots. Distribution of latency according to number of RSUs and traffic density compared to latency requirement of 20 msec

the latency requirement. In scenarios with low vehicle density, even with a single RSU, applications demanding a 20 msec latency are satisfactorily supported. However, as vehicle density escalates, latencies surge beyond the 20 msec threshold; nonetheless, increasing the RSU count brings about an overall latency reduction below 20 msec.

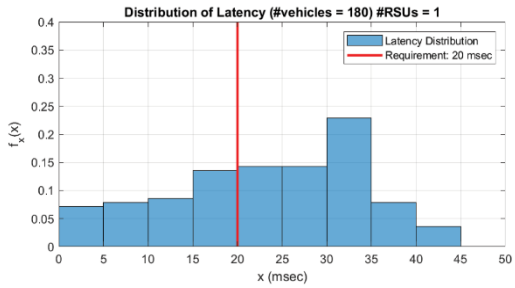

(a) 1 RSU and 30 vehicles/direction (without congestion control)

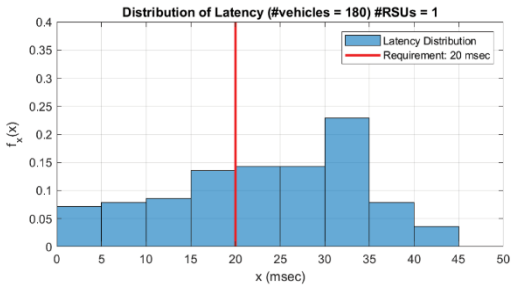

(b) 1 RSU and 30 vehicles/direction (with congestion control)

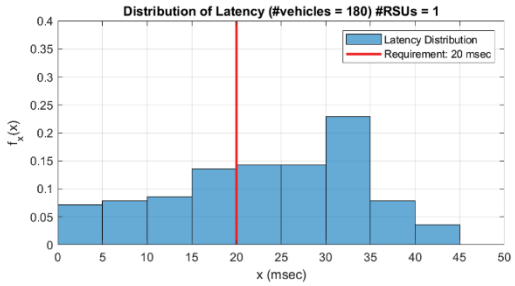

(c) 2 RSUs and 30 vehicles/direction (without congestion control)

Figure 37. Plots. Distribution of latency according to the presence of a congestion control mechanism

The outcomes depicted in Figure 36 are obtained from simulations conducted without the implementation of a congestion control mechanism, leading to elevated latency values in the case of higher vehicle density. To assess the most challenging conditions, we considered a heightened vehicle density ($\lambda = 30$, equivalent to a total of 180 vehicles) with a single RSU. In the absence of a congestion control mechanism, as shown in Figure 36a, latency far surpasses the 20 msec benchmark. Upon integrating a congestion control mechanism, latency for the majority of vehicles reduces below the 20 msec, as illustrated in Figure 36a. Interestingly, when both a congestion control mechanism and two RSUs are incorporated, an additional reduction in latency is observed, as highlighted in Figure 36a.

The subfigures comprising in Figure 38 provide insights into the PDR across various vehicle densities and distinct RSU counts. The vertical comparison within a single column reveals that heightened vehicle density corresponds to diminished PDR, while the horizontal comparison in a

singular row demonstrates that an increased RSU count contributes to an elevated PDR and higher reliability. The augment in RSUs translates to a greater pool of resources, thereby influencing the outcome. Significantly, the mean PDR for all vehicles within a given configuration is indicated by the green vertical line.

We consider the following assertion to be secure: even within the 30-MHz configuration, tasks necessitating a 100 msec latency can be accommodated across all situations. However, as λ increases, despite the implementation of 3 RSUs and a congestion control mechanism, certain vehicles still experience latencies surpassing 20 msec. This suggests that exceptionally dense vehicular populations might result in elevated latencies for certain vehicle segments, surpassing the 20 msec threshold. Consequently, this implies that in the 30-MHz spectrum setting, although nearly all other message types outlined in Table 1 can be facilitated, the 'V2V critical BSM' may not operate effectively with just a single RSU in scenarios characterized by high traffic density.

Verification via Driving Simulation

We are in the process of creating diverse driving simulation scenarios to test the message types outlined in Table 3. As depicted in Figure 4, the significant innovation of this research lies in the *integration* of a driving simulator and a C-V2X simulator. The outcomes derived from the current findings pertaining to latency and PDR underscore a crucial point: even in a 30 MHz configuration with heightened vehicular densities, the utilization of a congestion control mechanism ensures the reception of critical BSMs. The manner in which a vehicle acquires a BSM with minimal latency and subsequently takes essential measures to avert an imminent collision is elucidated through the driving simulator. The typical arrangement for our driving

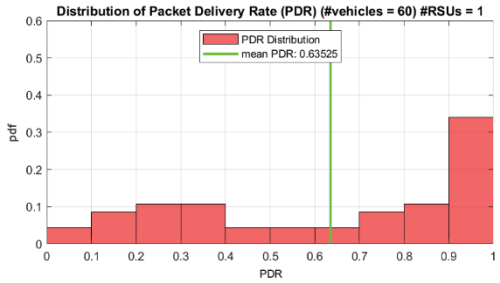

(a) 1 RSU and 10 vehicles/direction

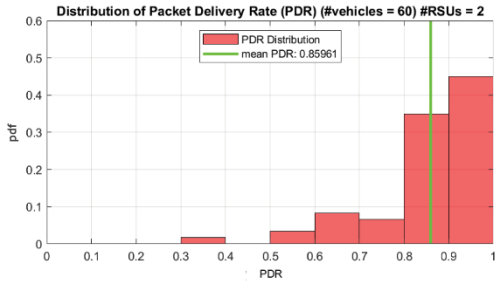

(b) 2 RSUs and 10 vehicles/direction

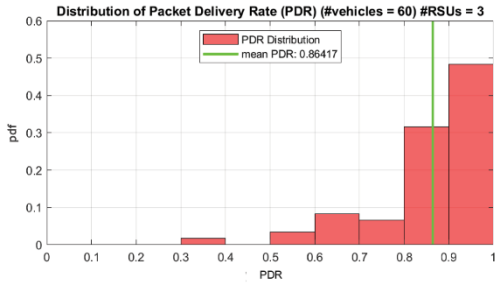

(c) 3 RSUs and 10 vehicles/direction

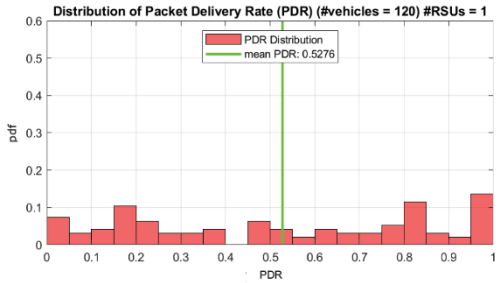

(d) 1 RSU and 20 vehicles/direction

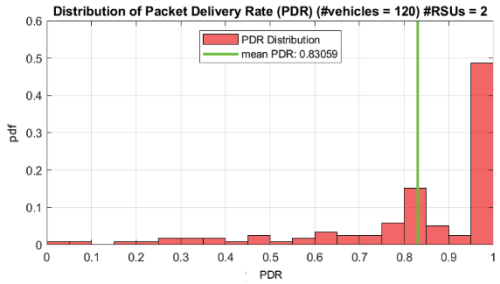

(e) 2 RSUs and 20 vehicles/direction

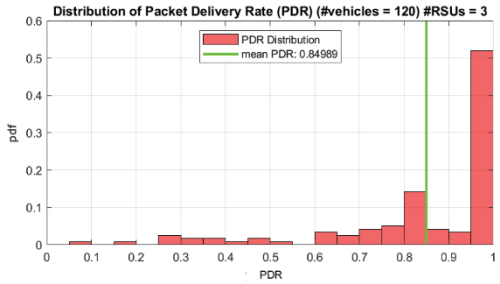

(f) 3 RSUs and 20 vehicles/direction

Figure 38. Plots. Distribution of PDR according to number of RSUs and traffic density compared to latency requirement of 20 msec

simulator involves a human participant situated in front of a custom-built driving simulator unit. This setup includes four monitors, a steering wheel, and pedals, effectively simulating the car's windshield, directional controls, and acceleration/braking actions.

Figure 39 illustrates the proposed driving simulation setup for the verification. The driven vehicle (the vehicle-of-interest" or "VoI" hereafter) is put into the following scenario where

continued exchange of V2V BSM via C-V2X can improve safety. The VoI is put onto a 2-lane road: i.e., a single lane per direction. The driver cares to pass the large trailer truck in front of the VoI, which blocks the driver's sight of the other-direction lane. We designed the simulation that because of the sight blockage, an attempt to pass the truck causes a *near crash* with another vehicle approaching from the other lane (the "vehicle-to-crash" or "VtC"). The assumption here (which is very realistic) is that if the VoI and VtC have successfully exchanged BSMs, the near crash can be avoided by the driver being able to refrain from the pass with the VtC approaching.

Figure 39. Photo. "Do not pass" warning scenario for V2V BSM test

Chapter 6. Conclusions

This project was devoted to investigating various spectrum options for Georgia's connected vehicle infrastructure, which has thus far been primarily based on DSRC, as a response to the nationwide concern on a reduced amount of spectrum due to the latest decision by the federal government.

The key findings can be summarized as:

- When considering the possibility of operating V2X communications in an unlicensed band where Wi-Fi already resides as a primary user, Wi-Fi-to-V2X interference is much higher than the opposite-direction interference. Thus, V2X seems to necessitate proper mechanisms to mitigate the interference in order to be operated in coexistence with Wi-Fi.
- From the technical perspective, it seems feasible that V2X communications use the 4.9 GHz Public Safety Band as long as a certain separation distance is guaranteed from the public safety users. It remains to be seen if the idea can be supported from the legislative context by the State of Georgia.
- In an attempt to assist GDOT regarding the nationwide possibility of transition to C-V2X from DSRC, this research developed three avenues of experimental platforms: viz., computer simulations, in-lab test, and field test.
- As part of this research, the team responds to the ITSA in identification of message types that can be supported by the reduced 30 MHz of bandwidth in the 5.9 GHz band. The

nominal 100 msec of latency requirement seems feasible to fulfill by using Release 15 LTE-V2X.

A list of published (and in-press) articles based on the findings from this project follows:

- D. Sunuwar and S. Kim, "What Safety Messages Can C-V2X Support?," in Proc. IEEE Intelligent Vehicles Symposium (IV) 2024, To appear.
- D. Sunuwar and S. Kim, "Cross-Layer Performance Evaluation of C-V2X," in Proc. IEEE Southeast Conference (SoutheastCon) 2024, To appear.
- L. Thompson and S. Kim, "In-lab implementation of DSRC PHY layer," in Proc. IEEE Southeast Conference (SoutheastCon) 2024, To appear.
- Z. Reyes, S. Kim, and D. Sunuwar, "Dangerous cars need to go first," in Proc. IEEE Vehicular Technology Conference (VTC) 2023 Fall.
- D. Sunuwar, S. Kim, and Z. Reyes, "Is 30 MHz enough for C-V2X?," in Proc. IEEE Vehicular Technology Conference (VTC) 2023 Fall.
- M. F. R. Khan and S. Kim, "On the feasibility of 4.9 GHz public safety band as spectrum option for internet of vehicles," in Proc. IEEE International Conference on Electronics, Information, and Communication (ICEIC) 2022.

References

3GPP. 2022. "5G; Service requirements for enhanced V2X scenarios." *ETSI TS 122186.*

3GPP. 2022. "5G; Study on channel model for frequencies from 0.5 to 100 GHz." ETSI TR 138901.

3GPP. 2022. "LTE; 5G Overall description of Radio Access Network (RAN) aspects for Vehicle-to-everything (V2X) based on LTE and NR." ETSI TR 137985.

3GPP. 2022. "LTE; Evolved Universal Terrestrial Radio Access (E-UTRA); Physical layer procedures." ETSI TS 136213.

3GPP. 2023. "LTE; Evolved Universal Terrestrial Radio Access (E-UTRA); User equipment (UE) radio transmission and reception." ETSI TS 136101.

—. 2016. "Study on LTE-based V2X Services; (Release 14)." *3GPP TR 36.885 V14.0.0.*

—. 2022. "Universal Mobile Telecommunications System (UMTS); LTE; Proximity-based services (ProSe); Stage 2." *ETSI TS 123303.*

5GAA. 2019. "Update on C-V2X Deployment in China."

5GCAR. 2019. "Intermediate Report on V2X Business Models and Spectrum." *5GCAR/D2.2.*

90.1213, CFR. 2023. *Code of Federal Regulations.* https://www.ecfr.gov/current/title-47/chapter-I/subchapter-D/part-90/subpart-Y/section-90.1213.

90.1215, CFR. 2023. *Code of Federal Regulations.* https://www.ecfr.gov/current/title-47/chapter-I/subchapter-D/part-90/subpart-Y/section-90.1215.

90.210, CFR. 2023. *Code of Federal Regulations.* https://www.law.cornell.edu/cfr/text/47/90.210.

90.523, CFR. 2023. *Code of Federal Regulations.* https://www.ecfr.gov/current/title-47/chapter-I/subchapter-D/part-90/subpart-R/section-90.523.

A. Bazzi, G. Cecchini, M. Menarini, B. M. Masini and A. Zanella. 2019. "Survey and perspectives of vehicular Wi-Fi versus sidelink cellular- V2X in the 5G Era." *Future Internet.*

A. I. Abu-Khadrah, A. Zakaria, M. Othman, and M. S. Zin. 2017. "Enhance the performance of EDCA protocol by adapting contention window." *Springer Wireless Personal Communications,.*

A. Mansouri, V. Martinez and J. Harri. 2019. "A First Investigation of Congestion Control for LTE-V2X Mode 4." *Proc. Annual Conf. Wireless On-demand Netw. Syst. Services (WONS) 2019.*

A. Nabil, K. Kaur, C. Dietrich and V. Marojevic. 2018. "Performance Analysis of Sensing-Based Semi-Persistent Scheduling in C-V2X Networks." *Proc. IEEE Veh. Technol. Conf. (VTC) Fall-2018.*

AASHTO. 2019. "State DOTs sign letter supporting preservation of 5.9 GHz spectrum."

Almeida, T. T., L. de C. Gomes, F. M. Ortiz, Junior, J. G. R., and L. H. M. K. Costa. 2018. "IEEE 802.11p performance evaluation: simulations vs. real experiments." *IEEE ISTC.*

B. Rinehart, D. Eierman. 2010. "4.9 GHz public safety broadband spectrum: Overview of technical rules and step-by-step licensing instructions."

Bianchi, G. 1998. "IEEE 802.11--Saturation throughput analysis." *IEEE Communications Letters* 12 (2).

Bianchi, G. 2000. "Performance analysis of the IEEE 802.11 distributed coordination function." *IEEE Journal on Selected Areas in Communications* 18 (3).

C. Zoghlami, R. Kacimi, and R. Dhaou. 2022. "5G-enabled V2X communications for vulnerable road users safety applications: A review." *Wireless Networks.*

CAMP. 2017. *SPaT challenge verification document.* ver. 1.2.

Cheng, B., H. Lu, A. Rostami, M. Gruteser, and J. B. Kenney. 2017. "Impact of 5.9 GHz spectrum sharing on DSRC performance." *IEEE VNC.*

Cho, S. Kim and Y. J. 2013. "Adaptive transmission opportunity scheme based on delay bound and network load in IEEE 802.11e wireless LANs." *J. Appl. Res. Technol.*

D. Sunuwar, S. Kim, Z. Reyes. 2023. "Is 30 MHz enough for C-V2X?" *Proc. IEEE Vehicular Technology Conference (VTC) 2023 Fall.* IEEE.

Dietrich, S. Kim and C. 2018. "A novel method for evaluation of coexistence between DSRC and Wi-Fi at 5.9 GHz." *Proc. IEEE Globecom.*

ElBatt, T., S. K. Goel, G. Holland, H. Krishnan, and J. Parikh. 2006. "Cooperative collision warning using dedicated short range wireless communications." *ACM VANET.*

ETSI. 2018. "Intelligent Transport Systems (ITS); Congestion Control Mechanisms for the C-V2X PC5 interface; Access layer part." *ETSI TS 103574.*

Fallah, Y. P., C. I. Huang, R. Sengupta, and H. Krishnan. 2010. "Analysis of information dissemination in vehicular ad-hoc networks with application to cooperative vehicle safety systems." *IEEE Trans. Veh. Technol.* 60 (1).

Fapojuwo, K. Ashrafuzzaman and A. O. 2018. "Efficient and agile CSMA in capillary M2M communication networks." *IEEE Access.*

FCC, US. 2019. "In the matter of use of the 5.850-5.925 GHz band." Notice of Proposed Rulemaking, ET Docket No. 19-138, FCC 19-129.

Forster, T. Karunathilake and A. 2022. "A survey on mobile road side units in VANETs." *MDPI Vehicles.*

GDOT. 2021. "A pocket reference to Georgia's transportation data 2021."

Gungor, B. E. Bilgin and V. C. 2013. "Performance comparison of IEEE 802.11 p and IEEE 802.11 b for vehicle-to-vehicle communications in highway, rural, and urban areas." *Hindawi Int. J. Veh. Technol.*

Huang, C. I., Y. P. Fallah, R. Sengupta, and H. Krishnan. 2010. "Intervehicle transmission rate control for cooperative active safety system." *IEEE Transactions on Intelligent Transportation Systems* 12 (3).

IA2, CFR. 2023. *Code of Federal Regulations.* https://www.ecfr.gov/current/title-47/chapter-I/subchapter-A/part-2.

IEEE. 2010. *802.11p-2010 - IEEE Standard for Information technology– Local and metropolitan area networks– Specific requirements– Part 11: Wireless LAN Medium Access Control (MAC) and Physical Layer (PHY) Specifications Amendment 6: Wireless Access in Vehicular Envir.* IEEE.

IEEE. 2011. "IEEE 1609.15010, IEEE standard for wireless access in vehicular environments (WAVE)—multi-channel operation."

IEEE. 2016. "IEEE 802.11-2016 - IEEE Standard for Information technology– Telecommunications and information exchange between 14 systems Local and metropolitan area networks–Specific requirements - Part 11: Wireless LAN MAC and PHY Specifications." (IEEE).

J. W. Tantra, C. H. Foh, and A. B. Mnaouer. 2005. "Throughput and delay analysis of the IEEE 802.11e EDCA saturation." *Proc. IEEE Int. Commun. Conf.*

Jornod, G., A. El Assaad, A. Kwochzek, and T. Kurner. 2019. "Packet interreception time modeling for high-density platooning in varying surrounding traffic density." *IEEE EuCNC.*

Kenney, J. Nov. 2018. "An update on V2X in the United States." *SIP-adus Workshop on Connected and Automated Systems.*

Khabazian, M, S Aissa, and M Mehmet-Ali. 2013. "Performance modeling of safety messages broadcast in vehicular ad hoc networks." *IEEE Transactions on Intelligent Transportation Systems* 14 (1).

Khan, I., G. M. Hoang, and J. Harri. 2017. "Rethinking cooperative awareness for future V2X safety-critical applications." *IEEE VNC.*

Kim, S. 2017. "Coexistence of wireless systems for spectrum sharing." *Ph. D. Dissertation* (Ph.D. Disertation, Virginia Tech).

Kim, S, and B.-J. Kim. 2020. "Reinforcement learning for accident riskadaptive V2X networking." *arXiv:2004.02379.*

Kim, S, and M Bennis. 2019. "Spatiotemporal analysis on broadcast performance of DSRC with external interference in 5.9 GHz band." *arxiv:192.02537.* https://arxiv.org/pdf/1912.02537.pdf.

Kim, S, and T Dessalgn. 2019. "Danger aware vehicular networking." *IEEE SoutheastCon.*

—. 2019. "Mitigation of civilian-to-military interference in DSRC for urban operations." *IEEE MILCOM.*

Kim, S. 2019. "Impacts of mobility on performance of blockchain in VANET." *IEEE Access.*

Kloiber, B., J. Harri, T. Strang, S. Sand, and C. R. Garcia. 2015. "Random transmit power control for DSRC and its application to cooperative safety." *IEEE Trans. Dependable Secur. Comput.* 13 (1).

L. Cao, S. Roy, and H. Yin. 2023. "Resource allocation in 5G platoon communication: Modeling, analysis and optimization." *IEEE Trans. Veh. Technol.*

Lei, X., and S. H. Rhee. 2019. "Performance analysis and enhancement of IEEE 802.11p beaconing." *EURASIP Journal on Wireless Communications and Networking* 2019 (61).

Liu, Z., Z. Liu, Z. Meng, X. Yang, L. Pu, and L. Zhang. 2016. "Implementation and performance measurement of a V2X communication system for vehicle and pedestrian safety." *Internat. J. Distributed Sensor Netw.* 12 (9).

LLC, Macrotrends. 2021. "Savannah metro area population 1950-2021."

Lobiyal, P. Patel and D. K. 2015. "A simple but effective collision and error aware adaptive back-off mechanism to improve the performance of IEEE 802.11 DCF in error-prone environment." *Springer Wireless Pers. Commun.*

M. Akdeniz, Y. Liu, M. Samimi, S. Sun, S. Rangan, T. Rappaport, and E. Erkip. 2014. "Millimeter wave channel modeling and cellular capacity evaluation." *IEEE J. Sel. Areas Commun.*

M. Al-Hubaishi, T. Alahdal, R. Alsaqour, A. Berqia, M. Abdelhaq, and O. Alsaqour. 2014. "Enhanced binary exponential backoff algorithm for fair channel access in the IEEE 802.11 medium access control protocol." *Int. J. Commun. Syst.*

M. Garcia, A. Molina-Galan, M. Boban, J. Gozalvez, B. Coll-Perales, T. Sahin, and A. Kousaridas. 2021. "A tutorial on 5G NR V2X communications." *IEEE Commun. Surveys Tutorials.*

M. Karaca, S. Bastani, and B. Landfeldt. 2017. "Modifying backoff freezing mechanism to optimize dense IEEE 802.11 networks." *IEEE Trans. Veh. Technol.*

N. O. Song, B. J. Kwak, J. Song, and M. Miller. 2003. "Enhancement of IEEE 802.11 distributed coordination function with exponential increase exponential decrease backoff algorithm." *Proc. IEEE Veh. Technol. Conf. (VTC) 2003-Fall.*

Nasr, M. Calabrese and A. 2020. "The 5.9 GHz band: Removing the roadblock to gigabit Wi-Fi." *FCC ECFS.*

NHTSA. 2023. *NHTSA Estimates Traffic Fatalities Continued to Decline in the First Half of 2023.* https://www.nhtsa.gov/press-releases/2023-Q2-traffic-fatality-estimates#:~:text=An%20estimated%2019%2C515%20people%20died,and%20second%20quarters%20of%202023.

—. 2016. "Proposed rule would mandate vehivle-to-vehicle (V2V) communication on light vehicles, allowing cars to 'talk' to each other to avoid crashes, NHTSA-3156." December. https://one.nhtsa.gov/About-NHTSA/Press-Releases/ci.nhtsa_v2v_proposed_rule_12132016.print.

—. 2006. "The 100-car naturalistic driving study: Phase II -- Results of the 100-car field experiment." *DOT HS 810 593.*

NTIA, US. 2023. *US Frequency Allocation Chart.* https://www.ntia.doc.gov/files/ntia/publications/2003-allochrt.pdf.

O'Driscoll, B. McCarthy and A. 2022. "Adapting the Resource Reservation Interval for Improved Congestion Control in NR-V2X." *Proc. IEEE Int. Symp. World Wireless Mobile Multimedia Netw. (WoWMoM).*

O'Hara, S. 2000. "4.9 GHz mask issues." Prepared for NPSTC Petition for Reconsideration 3rd Report & Order, FCC WTB Docket 00-32.

Qiu, H, I Ho, C Tse, and Y Xie. 2014. "Technical report: A methodology for studying 802.11p VANET." *arXiv:1410.3978.* https://arxiv.org/ftp/arxiv/papers/1410/1410.3978.pdf.

R. Moraes, P. Portugal, F. Vasques, and R. F. Custodio,. 2010. "Assessment of the IEEE 802.11e EDCA protocol limitations when dealing with realtime communication." *EURASIP J. Wirelss Commun. Netw.*

Rendaa, M. E., G. Restaa, P. Santi, F. Martelli, and A. Franchini. 2016. "IEEE 802.11p VANets: experimental evaluation of packet inter-reception time." *Elsevier Comput. Commun.* 75.

S. Kim, E. Visotsky, P. Moorut, K. Bechta, A. Ghosh, and C. Dietrich. 2017. "Coexistence of 5G with the incumbents in the 28 and 70 GHz bands." *IEEE J. Sel. Areas Commun.*

S. Y. Lien, D. J. Deng, H. L. Tsai, Y. P. Lin, and K. C. Chen. 2017. "Vehicular radio access to unlicensed spectrum." *IEEE Wireless Commun.*

SAE. 2022. "LTE-V2X deployment profiles and radio parameters for single radio channel multi-service coexistence." *J3161.*

—. 2020. "V2X communications message set dictionary." *J2735.*

SAE. 2022. "Vehicle level validation test procedures for V2V safety communications." J3161/1A.

Son, S., and K.-J. Park. 2019. "BEAT: beacon inter-reception time ensured adaptive transmission for vehicle-to-vehicle safety communication." *MDPI Sensors* 19 (14).

Song, C. 2017. "Performance analysis of the IEEE 802.11p multichannel MAC." *MDPI Sensors.*

Stanica, R, E Chaput, and A Beylot. 2014. "Reverse back-off mechanism for safety vehicular ad hoc networks." *Elsevier Ad Hoc Networks* 16.

Torrent-Moreno, M., J. Mittag, P. Santi, and H. Hartenstein. 2009. "Vehicle-tovehicle communication: Fair transmit power control for safety-critical information." *IEEE Transactions on Vehicular Technology* 58 (7).

US Department of Transportation. 2017. "Vehicle-to-vehicle communication technology, V2X Fact Sheet." July. Available: https://www.nhtsa.gov/sites/nhtsa.dot.gov/files/documents/v2v fact sheet 101414 v2a.pdf.

US FCC. 2019. "Dedicated short range communications (DSRC) service." April. Available: https://www.fcc.gov/wireless/bureaudivisions/mobility-division/dedicated-short-range-communicationsdsrc-service.

US FCC. Dec. 2019. *In the matter of use of the 5.850-5.925 GHz band.* Notice of Proposed Rulemaking, ET Docket No. 19-138.

USDOT. 2023. "CV273: Introduction to SPaT / MAP messages." *Module 62 - CV273.*

—. 2009. "Speed concepts: Informational guide." *FHWA-SA-10-001.*

USFCC. 2021. "Dissenting statement of commissioner Brendan Carr: Re: Amendment of Part 90 of the Commission's Rules, Order, WP Docket No. 07-100." FCC21-66.

Vere-Jones, D. Daley and D. 2013. "An Introduction to the Theory of Point Processes: Volume I: Elementary Theory and Methods." *Springer Probability and its Applications.*

W. Manda, S. H. Steiner, R. J. MacKay, and A. R. Hilal. 2019. "Using telematics data to find risky driver behaviour." *Accident Analysis & Prevention.*

W.-Y. Lin, M.-W. Li, K.-C. Lan, and C.-H. Hsu. 2010. "A comparison of 802.11a and 802.11p for V-to-I communication: A measurement study." *Proc. Int. Conf. Heterogeneous Netw. Quality, Reliability, Security and Robustness.*

Wang, Xiao, S Mao, and M. X. Gong. 2017. "An overview of 3GPP cellular vehicle-to-everything standards." *GetMobile: Mobile Computing and Communications* 21 (3): 19-25.

Wei, R. 2022. "Performance analysis of semi-persistent scheduling throughput in 5G NR-V2X: A MAC perspective." *arXiv:2208.10653v1.*

WTOC. 2021. *Police to interview driver of semi involved in crash on I-95 near I-16.* https://www.wtoc.com/2021/05/10/police-searching-semi-involved-crash-i-near-i-/.

Yao, Y, L Rao, and X Liu. 2013. "Performance and reliability analysis of IEEE 802.11p safety communication in a highway environment." *IEEE Transactions on Vehicular Technology* 62 (9).

Yin, X, X Ma, and K. S. Trivedi. 2013. "An interacting stochastic models approach for the performance evaluation of DSRC vehicular safety communication,." *IEEE Transactions on Computers* 62 (5).

Z. Reyes, S. Kim, D. Sunuwar. 2023. "Dangerous cars need to go first." *Proc. IEEE Vehicular Technology Conference (VTC) 2023 Fall.* IEEE.